Stable Majoron Radiation in the Type 1 See-Saw Mechanism and Its Hypothetical Detection at the LHC

In partial fulfillment of the requirements for the Degree of

Master of Science-Physics

Gustavo Adolfo Ardila Tafurth

University of Heidelberg
Faculty of Physics and Astronomy

Advisors
Werner Rodejohann. Ph.D
Andrés Florez. Ph.D (Univ. De los Andes, Kolumbien)

Heidelberg Germany
2020

To my dad.

Acknowledgments

I would like to thank both my advisors, Dr. Andrés Florez for his unconditional and extraordinary support not only in this thesis process but through my entire career and Prof. Werner Rodejohann for his support and advise during this project. Secondly, I would like to thank Nicolas Vergara and Nathalia Cardona for their support, faith and for those meetings full of physics and knowledge; you really motivated me to keep pushing forward. Thirdly, I would like to thank all members of the High Energy Physics-Pheno research group at Universidad de los Andes for their wonderful collaboration, you supported me greatly and were always willing to help me. Consequently, I would also like to thank my friends for their friendship and help during this whole process, you were always there to help me and supported me unconditionally. Finally, I would like to thank my parents for their love, faith and patience through these last two years, you kept me on path and were always there when I needed you the most.

Erklärung:

Ich versichere, dass ich diese Arbeit selbstständig verfasst habe und keine anderen als die angegebenen Quellen und Hilfsmittel benutzt habe.

Heidelberg, den (Datum) **30.09.2020** .... Gustavo Adolfo Ardila Tafurth

Contents

1. Introduction

The Standard Model of particle physics (SM) has been, together with General Relativity, one of the most succesful theories in physics. The SM mixes relativistic quantum mechanics with continuum field theory; it describes the behavior of elementary particles and their interactions [1]. The interactions of particles are described through the principle of gauge invariance, which emerge as consequence of the study of fundamental symmetries satisfied by particle fields. The easiest example of gauge invariance comes from electromagnetism where the 4-potential, A_μ, can be transformed by the means of Equation 1.1, such that the electric and magnetic fields remain the same.

$$A_\mu \rightarrow A'_\mu = A_\mu + \partial_\mu \lambda \tag{1.1}$$

The choice of a given λ fixes the gauge and implies that some components of the potential could vanish. One example of this is the Lorenz gauge, where we set $\partial_\mu A^\mu = 0$. This basic symmetry of the potential can be understood in terms of Lie groups [2], namely the U(1) group, where its elements can be understood as continuous phase rotations. If we generalize the fact that each interaction should follow some gauge invariance, under a certain Lie group, we will be able to construct a field theory for that interaction. Furthermore, if we now quantize the interaction fields, we will have a Quantum Field Theory (QFT) for it.

The SM is the most complete Lorentz and gauge invariant theory to describe the quantum realm. It includes three of the four main interactions and associates to them vector bosons, such as $\gamma, W^\pm, Z^0, g_i$. The $W^\pm$, γ and Z^0 are the three gauge bosons associated with the weak interaction, and arise from the $SU(2)_L \times U(1)_Y$ symmetry, while the g_i are the eight gluons associated with the strong interaction, and arise from the $SU(3)_C$ Lie group. It is worth noticing that the subscripts L, Y and C arise from the conserved isospin, hypercharge and color quantum numbers. Therefore, the SM can be written in a single gauge group as

$$G_{SM} = SU(3)_C \times SU(2)_L \times U(1)_Y, \tag{1.2}$$

where the fermion fields transform in the fundamental representation, while the gauge fields transform in the adjoint representation. However, at high energies the electroweak $SU(2)_L \times U(1)_Y$ gauge group behave as a single interaction, breaking to the $U(1)_Q$ group. [1]. This symmetry breaking occurs by the means of the so called Higgs mechanism, whose interactions with matter give rise to mass terms that violate gauge invariance under transformations of the electroweak gauge group.

Even though the SM has been successful in explaining a broad variety of phenomena, there are some experimental and phenomenological observations that cannot be explained within its formalism, leaving many open questions related to topics such as quantum triviality[3], Higgs boson mass finiteness [4], matter-antimatter asymmetry [5], neutrino oscillations and mass [6],

---

[1]The subscript Q denotes electric charge

quantum gravity [7], etc.

Many theories have been proposed to explain each of these problems, from Supersymmetric Models [8] and Grand Unified Theories [9] (GUTs) to String Theory [10]. Some of these theories, specially those explaining neutrino masses, include a U(1) extension to the theory that predicts the existence of massive right-handed neutrinos, whose mass can be explained within three possible mechanisms, referred to as Seesaw mechanisms [11]. As there are many possible U(1) extensions of the SM, we focus on scenarios where the so called B-L symmetry is conserved. For example, this type of models can explain the observed matter-anti-matter asymmetry in the universe (leptogenisis) [12].

One of the simplest theories to explain the generation of neutrino masses, is the Singlet Majoron Model [13]. In this model, one introduces a singlet scalar field, φ, that couples only to fields charged under $U(1)_{B-L}$ symmetry group. After Spontaneous Symmetry Breaking, it is possible to use a Kibble parametrization for the scalar field, such that [14]

$$\varphi = \frac{1}{\sqrt{2}}(f + A + iJ) \tag{1.3}$$

In Equation 1.3 A and J are real scalar fields. In this project we focus on how the Goldstone mode of φ, J, couples to matter. Additionally, a preliminary feasibility study for the production of this process at the CERN's Large Hadron Collider (LHC) is presented.

The right-handed neutrino states have been object of study at many particle physics experiments such as IceCube [15], as well as the CMS [16] and ATLAS [17] experiments at CERN's Large Hadron Collider (LHC). The most recent experimental searches have considered Heavy Neutrino (HN) production via Drell-Yan (DY) mechanisms as the main production mechanism. However, no signal of these neutrinos has been found until now [1]. Since in no signs of physics beyond the SM has been observed yet at the LHC, theoretical and phenomenological studies have been published in recent years [18, 19, 20], proposing new models and analysis techniques to detect new particles. For example, the Vector Boson Fusion (VBF) topology, has been proposed in several articles as an alternative and interesting mechanism to study regions of difficult experimental access at the LHC [21, 22, 23].

The VBF process result from the fusion of two vector bosons $(\gamma, Z^0, W^\pm)$ radiated from two quarks. The main experimental features VBF process are the production of two energetic jets with a large pseudorapidity gap, located on opposite hemispheres of the cilindrical-shaped particle detector, with large reconstructed dijet mass. The associated production cross sections VBF processes are $10^{-1} - 10^3$ smaller with respect to standard DY production. Nevertheless, the requirement of VBF topology allows a background suppression ranging from $10^{-3} - 10^{-6}$, depending on the background, allowing VBF to be competitive with respect respect to other searches considering standard Drell-Yan or W-meadiated production mechanisms. n this dissertation we study the hypothetical production of unstable HN in association with Majorons at the LHC. We consider two possible production mechanisms, through W-mediated process and through VBF. In the model, we consider the Majoron as a stable radiated boson from the HN, becoming a canonical Dark Matter (DM) candidate. A representative Feynman diagram for the production of the signal

model under study through VBF is presented in 1.1[2].
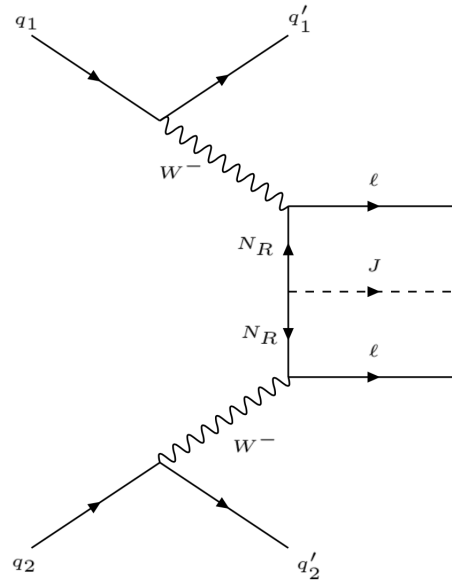

Figure 1.1: Production of a Majoron via indirect VBF

As the Majoron, J, origins from theories that extend the SM to explain neutrino masses, its finding can be an important target at the CMS and ATLAS experiments, as it can become, together with the new neutrino states, a perfect DM candidate. Nevertheless, the production of this particle at colliders has not been largely studied. The work presented in this disertation aims to be a first theoretical and phenomenological approach to calculate both matrix elements and cross sections for the J production via DY, W and VBF channels.

---

[2]Feynman diagrams are made using the online tool `https://feynman.aivazis.com`

2. Theoretical Framework

The Standard Model of particle physics (SM) is a relativistic quantum field theory that encapsulates our knowledge and understanding of the fundamental particles and how they interact by the means of the electromagnetic, strong and weak interactions. Within this formalism particles are modeled as quanta of fields that permeate space-time and, according to their spin values, are divided into two families: Fermions and bosons. In the SM fermions are spin-$\frac{1}{2}$ particles that constitute matter and interact via boson exchange [24]. These bosonic exchanges arise as consequence of gauge invariance of the fermion Lagrangian under the gauge group

$$SU(3)_C \times SU(2)_L \otimes U(1)_Y, \tag{2.1}$$

where the subscripts C, L and Y denote the color charge, left-handed chirality and weak hypercharge respectively. Additionally, the SM describes how the electromagnetic and weak interactions unify into the electroweak interaction, the origins of quarks due to color interactions and also how particles gain mass via Spontaneous Symmetry Breaking (SSB).

To fully understand all these concepts mentioned before, it is useful to make a brief reminder of the theory underlying the SM, starting with Quantum Electrodynamics (QED) and Quantum Chromodynamics (QCD) before making a longer summary of the weak interaction and SSB.

2.1 Quantum Electrodynamics

Before the discovery of QED Dirac discovered that the dynamics of spin-$\frac{1}{2}$ particles, which are modeled by a 4-component spinor ψ, are dictated by the equation that now holds his name [25]

$$i\gamma^\mu \partial_\mu \psi - m\psi = 0, \tag{2.2}$$

where γ^μ are the four 4×4 matrices that arise from the Clifford algebra given in Equation 2.3.

$$\{\gamma^\mu, \gamma^\nu\} = 2\eta^{\mu\nu} \tag{2.3}$$

The most general solution of Equation 2.2 is given by plane superposition and positive energy spinors u, v which are associated to particles and antiparticles respectively. These solutions take the form

$$\psi(x) = \sum_{r=1}^{2} \int \frac{\mathrm{d}^3 p}{(2\pi)^3} \frac{1}{\sqrt{2E_p}} [c_r(p)u_r(p)e^{-ipx} + d_r^*(p)v_r(p)e^{ipx}], \tag{2.4}$$

where r is an index indicating the two positive energy spinors for u and v [26]. In addition to ψ, it was later found that one can construct an additional, linearly independent field given by $\bar{\psi} = \psi^\dagger \gamma^0$.

With these two fields, one can construct a Lagrangian for a free Dirac spinor [27]

$$\mathcal{L} = i\bar{\psi}\gamma^\mu \partial_\mu \psi - m\bar{\psi}\psi. \tag{2.5}$$

Then, it is straightforward to note that this Lagrangian remains invariant under global U(1) transformations given by

$$\begin{aligned}
\psi &\to \psi' = e^{i\theta}\psi \\
\bar{\psi} &\to \bar{\psi}' = e^{-i\theta}\bar{\psi}.
\end{aligned} \tag{2.6}$$

One can then use Noether's theorem to obtain a conserved current [28], which is given by

$$J^\mu = ie\bar{\psi}\gamma^\mu \psi \tag{2.7}$$

Now that a conserved current has been found, one can promote the U(1) transformations to a local set up [29]. In other words, the maps

$$\begin{aligned}
\psi &\to e^{i\theta(x)}\psi = (1 + i\theta(x))\psi \\
\bar{\psi} &\to e^{-i\theta(x)}\bar{\psi} = (1 - i\theta(x))\bar{\psi}
\end{aligned} \tag{2.8}$$

have to be considered. With these transformations, one obtains that the mass term of the Lagrangian remains invariant while the kinetic term breaks it as the derivative does not transform properly as seen in Equation 2.10.

$$\begin{aligned}
\partial_\mu \psi' &= e^{i\theta(x)}(i\partial_\mu \theta)\psi + e^{i\theta}\partial_\mu \psi \tag{2.9} \\
&\neq e^{i\theta} \tag{2.10}
\end{aligned}$$

To solve this problem one introduces a U(1) covariant derivative, which introduces a vector field A_μ such that one can replace

$$\partial_\mu \to D_\mu = \partial_\mu - ei A_\mu, \tag{2.11}$$

while the vector field simultaneously transforms in the adjoint representation

$$A_\mu \to A_\mu - \frac{1}{e}\partial_\mu \theta(x) \tag{2.12}$$

This being said, one can check that the conserved current given in Equation 2.7 arises naturally from the Lagrangian

$$\begin{aligned}
\mathcal{L} &= i\bar{\psi}\gamma^\mu D_\mu \psi - m\bar{\psi}\psi \tag{2.13} \\
&= i\bar{\psi}\gamma^\mu \partial_\mu \psi - m\bar{\psi}\psi - e\bar{\psi}\gamma^\mu \psi A_\mu \tag{2.14}
\end{aligned}$$

but coupled to the field A_μ. It is important to note that both fields $\bar\psi$ and ψ describe electrically charged fields, such that the last term in Equation 2.14 can be easily understood as the electromagnetic interaction of these fields mediated by the field A_μ [30]. Hence, one can infer that this vector field is the electromagnetic field, whose dynamics is governed by the Lagrangian given in Equation 2.15.

$$\mathcal{L} = -\frac{1}{4} F_{\mu\nu} F^{\mu\nu} \quad \text{with} \quad F_{\mu\nu} = \partial_\mu A_\nu - \partial_\nu A_\mu \tag{2.15}$$

Thus, if one wants to have a general U(1) gauge invariant Lagrangian that contains the dynamics for both fermions and the photon, one has to add the terms on Equations 2.14 and 2.15. This Lagrangian describes the whole theory underlying QED and is given by

$$\mathcal{L} = i\bar\psi\gamma^\mu\partial_\mu\psi - m\bar\psi\psi - \frac{1}{4}F_{\mu\nu}F^{\mu\nu} - \bar\psi\gamma^\mu\psi A_\mu \tag{2.16}$$

From this Lagrangian, one can obtain all possible electromagnetic phenomena after introducing the interacting term into the expression for the S matrix [31],

$$S^{(1)} = \exp\left[-ie\int \mathrm{d}^4 x\, T(\bar\psi\gamma^\mu A_\mu \psi)\right], \tag{2.17}$$

and performing a Taylor expansion of the exponential, as well as the corresponding Wick contractions [32]. From this expansion, one can deduce a simple set of rules that help to build the matrix elements associated to the electromagnetic phenomena at all orders in the expansion. These set of rules were first discovered by Richard Feynman and are referred to as Feynman rules [33]. For QED we obtain the following set of rules:

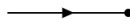- For every incoming fermion assign a spinor $u_s(p)$

Figure 2.1: Incoming fermion.

- For every incoming antifermion assign a spinor $\bar v_s(p)$

Figure 2.2: Incoming antifermion.

- For every incoming boson assign a polarization vector $\epsilon_r^\mu(p)$

Figure 2.3: Incoming boson.

- For every outgoing fermion assing a spinor $\bar{u}_s(p)$

Figure 2.4: Outgoing fermion.

- For every outgoing antifermion assign a spinor $v_s(p)$

Figure 2.5: Outgoing antifermion.

- For every outgoing boson assign a polarization vector $\epsilon^*_{\mu r}(p)$

Figure 2.6: Outgoing boson.

- All particles connect into a vertex. This vertex has a momentum space function given by $-ie\gamma^\mu$.

- For each internal fermion line assign a propagator $iS_F(q) = \frac{i(\gamma^\mu q_\mu + m)}{q^2 - m^2 + i\epsilon}$


Figure 2.7: Fermion internal line

- For each internal photon line assign a propagator $iD_{\mu\nu}(q) = \dfrac{-i\left(\eta_{\mu\nu} - (\xi - 1)\frac{q_\mu q_\nu}{q^2}\right)}{q^2 + i\epsilon}$. For simplicity we choose the Feynman gauge, such that the second term in the propagator vanishes.

Figure 2.8: Photon internal line

Note that there is an extra $i\epsilon$ factor in the propagators of both fermions and photons, and arises to ensure causality in the theory. In addition to these basic rules, it is possible to obtain an extra

one which arises from higher order terms. These terms generate diagrams like
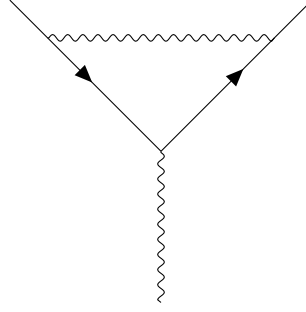
that contain extra internal lines and are known as loop diagrams. The momenta of the particles present in the loop are then integrated, giving us the final rule:

- For each loop present in a diagram, integrate over the momenta of the additional particle $\int \frac{\mathrm{d}^4 k}{(2\pi)^4}$.

However, these loop diagrams are divergent and require renormalization and regularization processes to take out these divergencies [34]. Additional topics like field quantization and the Gupta-Bleuler condition exceed the depth of this summary and references [28, 35] are recommended if the reader is interested.

2.2 Quantum Chromodynamics

Even though QED became the first quantum field theory that describes the electromagnetic interactions of fermions, it did not explain neither how quarks constitute nucleons nor how they hold together in the atomic nucleus or the origins of hadrons. The first approach to a correct theory was made by Gell-Mann, Nishijima and Pais when they introduced the Eightfold Way, an SU(3) gauge invariant theory that was based in flavor conservation to explain the origin of all hadrons. Nevertheless, their theory was quickly discarded after the discovery of the Δ^{++} and Ω^- resonances, as they explicitly violated the exclusion principle due to their quark content as seen in Equation 2.18, as well as from the discovery of the J/ψ resonance that indicated the presence of the charm quark [36, 37].

$$\left|\Delta^{++}\right\rangle = |uuu\rangle \quad \left|\Omega^-\right\rangle = |sss\rangle \tag{2.18}$$

Based on the clear incompatibility of the SU(3) flavor symmetry with the experimental data Nambu proposed the existence of a new quantum number, the color charge. This new symmetry modeled quarks as colour triplets of the form [38]

$$|\psi\rangle = \sum_i a_i C_i |\psi(p)\rangle; \quad C_1 = r = \begin{pmatrix} 1 \\ 0 \\ 0 \end{pmatrix} \quad C_2 = g = \begin{pmatrix} 0 \\ 1 \\ 0 \end{pmatrix} \quad C_3 = b = \begin{pmatrix} 0 \\ 0 \\ 1 \end{pmatrix} \tag{2.19}$$

such that hadrons can be considered to be color singlets. It is then straightforward to note that the color vectors span a 3D Hilbert space whose unitary transformations are given by SU(3)$_C$[1][39].

Hence, it is required to construct a SU(3)$_C$ gauge theory for quarks to explain the whole phenomena associated with the strong interaction. First, one has to note that SU(3) is a non abelian Lie group, contrary to the QED case, with Lie algebra

$$[T_i, T_j] = if_{ijk}T_k, \tag{2.20}$$

where f_{ijk} are the skew-symmetric structure constants and T_i are the 8 generators of the algebra[2]. In the fundamental representation these generators are proportional to the Gell-Mann matrices via $T_i = \frac{1}{2}\lambda_i$. These matrices are given in Equation 2.21.

$$
\lambda_1 = \begin{pmatrix} 0 & 1 & 0 \\ 1 & 0 & 0 \\ 0 & 0 & 0 \end{pmatrix} \quad
\lambda_2 = \begin{pmatrix} 0 & -i & 0 \\ i & 0 & 0 \\ 0 & 0 & 0 \end{pmatrix} \quad
\lambda_3 = \begin{pmatrix} 1 & 0 & 0 \\ 0 & -1 & 0 \\ 0 & 0 & 0 \end{pmatrix} \quad
\lambda_4 = \begin{pmatrix} 0 & 0 & 1 \\ 0 & 0 & 0 \\ 1 & 0 & 0 \end{pmatrix}
$$
$$
\lambda_5 = \begin{pmatrix} 0 & 0 & -i \\ 0 & 0 & 0 \\ i & 0 & 0 \end{pmatrix} \quad
\lambda_6 = \begin{pmatrix} 0 & 0 & 0 \\ 0 & 0 & 1 \\ 0 & 1 & 0 \end{pmatrix} \quad
\lambda_7 = \begin{pmatrix} 0 & 0 & 0 \\ 0 & 0 & -i \\ 0 & i & 0 \end{pmatrix} \quad
\lambda_8 = \frac{1}{\sqrt{3}} \begin{pmatrix} 1 & 0 & 0 \\ 0 & 1 & 0 \\ 0 & 0 & -2 \end{pmatrix}
\tag{2.21}
$$

As quarks are modelled as fermionic particles, their dynamics are contained in the Lagrangian [3] [40] given in Equation 2.22.

$$\mathcal{L} = i\bar{\psi}_c^f \gamma^\mu \partial_\mu \psi_c^f - m\bar{\psi}_c^f \psi_c^f \tag{2.22}$$

If one then considers the triplet behavior of quarks, one can obviate the color index such that the Lagrangian takes

$$\mathcal{L} = i\bar{\psi}_f \gamma^\mu \partial_\mu \psi_f - m\bar{\psi}_f \psi_f \tag{2.23}$$

With this Lagrangian it is then mandatory to check global invariance under $SU(3)_C$ transformations by considering the maps

$$\psi_f \rightarrow e^{i\alpha_a T_a} \psi_f \qquad\qquad \bar{\psi}_f \rightarrow \bar{\psi}_f e^{-i\alpha_a T_a} \tag{2.24}$$

As α_a are space-time independent parameters, the Lagrangian will remain invariant. Thus, after using Noether's theorem one obtains eight conserved currents which are given by Equation 2.25.

$$J_a^\mu = \bar{\psi}_f \gamma^\mu T_a \psi_f \tag{2.25}$$

After checking that Equation 2.22 is invariant under global $SU(3)_C$ transformations, it is then

---

[1]C denotes color charge.

[2]The structure constants take the role of the Levi-Civita density for SU(2).

[3]Here, Einstein summation convention has been used over the flavor (f) and color (c) indices.

mandatory to promote the symmetry transformations to a local setting. Hence, one maps

$$\psi_f \to \exp(ig_s\alpha_a(x)T_a)\psi_f \qquad\qquad \bar\psi_f \to \bar\psi_f \exp(-ig_s\alpha(x)T_a), \qquad (2.26)$$

and notes that the derivative term is non invariant. Following the same procedure done in QED, one defines the covariant derivative

$$D_\mu = \partial_\mu + ig_s T_a A_{a\mu}, \qquad (2.27)$$

where the A_a are the eight gauge bosons mediating the strong interaction, which are known as gluons. These gluons must transform via Equation 2.28. Note that there is an extra term in this transformation and can be explained by the non abelian behavior of the gauge group [14].

$$A_{a\mu} \to A_{a\mu} + \frac{1}{g_s}\partial_\mu\alpha_a - f_{abc}\alpha_b A_{c\mu} \qquad (2.28)$$

Additionally, one needs to introduce the gluon strength tensor to add a dynamical term for them in the total Lagrangian of the theory, which we call Quantum Chromodynamics (QCD) . This tensor takes the form
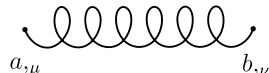
$$F_a^{\mu\nu} = \partial^\mu A_a^\nu + \partial^\nu A_a^\mu + g_s f_{abc} A_b^\mu A_c^\nu, \qquad (2.29)$$

such that the total QCD Lagrangian reads [30]

$$\mathcal{L} = i\bar\psi_f\gamma^\mu\partial_\mu\psi_f - m\bar\psi_f\psi_f + g_s J_a^\mu A_{a\mu} - \frac{1}{4}F_a^{\mu\nu}F_{\mu\nu}^a \qquad (2.30)$$

This Lagrangian describes all possible dynamics for processes regarding quarks and their interactions. However, the quantization procedure can be very complicated due to the non abelian behavior of the gluon field. Hence, one needs to introduce functional integral quantization and Faddeev-Popov ghost fields. For more insight on these topics, as well as renormalization of non abelian theories and asymptotic freedom, see [14, 31, 34, 41][ref:amateur,srednicki, schwartz, kleinert]. Given this Lagrangian, one can follow the same procedure than in QED to obtain the following set of Feynman rules [42, 43]
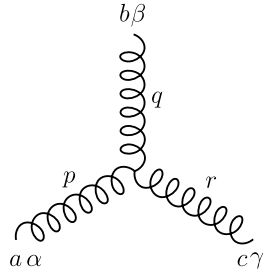
- Gluon propagator

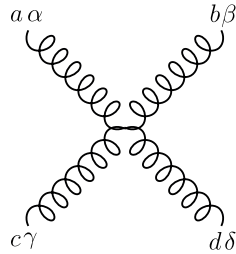$$-i\frac{\eta_{\mu\nu}\delta_{ab}}{p^2 + i\epsilon}$$

- Quark propagator

$$i\frac{\delta_{ab}}{\not{p} - m + i\epsilon}$$
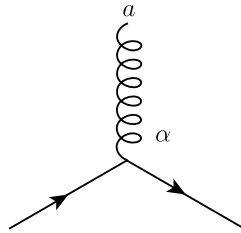
15

- 3 Gluon vertex factor

$$g_s f_{abc}[\eta^{\alpha\beta}(p-q)^\gamma + \eta^{\beta\gamma}(q-r)^\alpha + \eta^{\gamma\alpha}(r-p)^\beta]$$

- 4 Gluon vertex

$$-ig_s^2 f_{xac}f_{xbd}(\eta^{\alpha\beta}\eta^{\gamma\delta} - \eta^{\alpha\delta}\eta^{\beta\gamma})$$
$$-ig_s^2 f_{xad}f_{xbc}(\eta^{\alpha\beta}\eta^{\gamma\delta} - \eta^{\alpha\gamma}\eta^{\beta\delta})$$
$$-ig_s^2 f_{xab}f_{xcd}(\eta^{\alpha\gamma}\eta^{\beta\delta} - \eta^{\alpha\delta}\eta^{\beta\gamma})$$

- Quark-Gluon vertex factor

$$= ig_s \lambda^a \gamma^\alpha$$

2.3   The Weak Interaction

In the 1930's Fermi proposed that weak processes such as β decay could be explained by the means of two currents that interact in a single point as seen in Figure 2.9
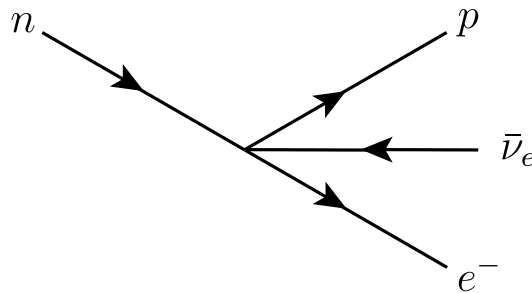

Figure 2.9: Graphical representation of Fermi's point-like interaction.

However, experimental phenomena proved that the interaction was not point-like and had to be mediated through a massive vector boson, contrary to QED. Around the 1950's Gell-Mann

and Nishijima formulated the quark model, based on Isospin and hypercharge conservation. This allowed physicists to understand the β decay as the process

$$d \rightarrow u + e^- + \bar{\nu}_e \tag{2.31}$$

Inspired by the isospin model, which was not exact for quarks, Fermi attempted to build an SU(2) gauge invariant theory for the weak interaction, where β decay is just one possible manifestation of it. He argued that quarks and leptons could be arranged into isospin doublets as $mu \approx m_d$ and $m_e << m_u$ (thus can be taken as negligible). These doublets are given by

$$q = \begin{pmatrix} u \\ d \end{pmatrix} \quad \ell = \begin{pmatrix} \nu_e \\ e \end{pmatrix} \tag{2.32}$$

The isospin assignation for each element of the doublets is then [4]

$$T_3 \left| u \right\rangle = \frac{1}{2} \left| u \right\rangle \quad T_3 \left| \nu_e \right\rangle = \frac{1}{2} \left| \nu_e \right\rangle \quad T_3 \left| d \right\rangle = \frac{-1}{2} \left| d \right\rangle \quad T_3 \left| e^- \right\rangle = \frac{-1}{2} \left| e^- \right\rangle \tag{2.33}$$

Based on Fermi's point-like interacting currents, a possible Lagrangian that describes the β decay can be taken to be

$$\mathcal{L} = i\bar{q}\gamma^\mu \partial_\mu q + i\bar{\ell}\gamma^\mu \partial_\mu \ell - m_q \bar{q}q - m_\ell \bar{\ell}\ell + \frac{G_F}{\sqrt{2}} u^\dagger d e^\dagger \nu_e, \tag{2.34}$$

where G_F is the Fermi coupling constant [5]

Nevertheless, in 1956 Yang and Lee proposed that as there was no experimental evidence showing the weak interaction to be invariant under parity transformations, a parity violating theory must not be discarded [6]. Their idea, though polemical and disregarded by physicists like Pauli, was proved right by Wu in 1957 after studying the decay of ^{6}0Co isotopes under a magnetic field [44]. She observed an excess of decay events on one specific direction of the applied magnetic field, contrary to the expected symmetrical distribution, implying that the weak interaction does not conserve parity.

The preference of an specific direction of decay in the weak interaction caused many physicists to look for solutions. Perhaps the most successful one was proposed by Feynman, where he considered that the theory could be explained via the introduction of vector-axial, or (V-A), currents as they are the only ones matching the experimental data given by Wu. The proposed currents take the form [45]

$$J^\mu = \frac{G_F}{\sqrt{2}} \bar{\psi}\gamma^\mu P_L \psi; \quad P_L = \frac{1}{2}(1 - \gamma_5) \tag{2.35}$$

---

[4]This assignation was later extended to up-like quarks (u, s, t), down-like quarks (d, c, b), electron-like leptons (e, μ, τ) and their corresponding neutrinos (ν_e, ν_μ, ν_τ).

[5]This constant was later understood as the weak coupling constant of an effective theory at low energies.

[6]We understand a parity transformation as mapping $\vec{x} \rightarrow -\vec{x}$ and $\vec{p} \rightarrow -\vec{p}$.

Note that using these (V-A) currents, obligates us to use a new representation of the gamma matrices, namely the Weyl (or chiral) representation, where they are given by [31, 42]

$$\gamma^0 = \begin{pmatrix} 0 & \mathbb{1} \\ \mathbb{1} & 0 \end{pmatrix} \quad \gamma^i = \begin{pmatrix} 0 & \sigma_i \\ -\sigma_i & 0 \end{pmatrix} \quad \gamma_5 = \begin{pmatrix} -\mathbb{1} & 0 \\ 0 & \mathbb{1} \end{pmatrix} \tag{2.36}$$

As γ_5 is diagonal, one can decompose a Dirac spinor in terms of the eigenstates of this matrix, known as left-handed and right-handed chiralities

$$\psi = \psi_L + \psi_R \tag{2.37}$$

As these eigenstates form a basis of the spinor space, one can define projectors as

$$P_L = \frac{1}{2}(1 - \gamma_5) P_R = \frac{1}{2}(1 + \gamma_5) \to P_L P_R = 0 \qquad P_{L/R}^2 = P_{L/R} \tag{2.38}$$

Based on this projections, one can check that (V-A) currents imply that only left-handed chiralities participate on the weak interaction[7]. Thus, the doublets previously defined in Equations 2.32 and 2.33 are only formed by these left-handed states. This being said, if we replace Dirac spinors in terms of Equation 2.37 we obtain that spinor dynamics is given now by

$$\mathcal{L} = i\bar{\psi}_L \gamma^\mu \partial_\mu \psi_L + i\bar{\psi}_R \gamma^\mu \partial_\mu \psi_R - m\bar{\psi}_R \psi_L - m\bar{\psi}_L \psi_R \tag{2.39}$$

Note that an SU(2) transformation like

$$\psi_L \to \psi'_L \propto \exp(i\alpha\gamma_5)\psi_L$$

will not leave the mass terms invariant, one says then that mass terms break gauge invariance. Additionally, note that as neutrinos only participate in weak processes, they can only posses left-handed chirality which means that they are massless.

As mass terms break gauge invariance, physicists like Weinberg, Salam, Feynman and Glashow started studying an analogous theory of the one originally proposed by Fermi, without including mass terms. In other words, they considered Lagrangians like

$$\mathcal{L} = i\bar{\psi}_L \gamma^\mu \partial_\mu \psi_L + i\bar{\psi}_R \gamma^\mu \partial_\mu \psi_R \tag{2.40}$$

where the left-handed chiralities are $SU(2)_L$ doublets [8] and the right-handed states are singlets. Hence, based on Equation 2.34 quark and lepton dynamics are given by

$$\mathcal{L} = i\bar{q}_L \gamma^\mu \partial_\mu q_L + i\bar{\ell}_L \gamma^\mu \partial_\mu \ell_L + i\bar{u}_R \gamma^\mu \partial_\mu u_R + i\bar{d}_R \gamma^\mu \partial_\mu d_R + i\bar{e}_R \gamma^\mu \partial_\mu e_R \tag{2.41}$$

where u_R, d_R and e_R are right-handed singlets for the up-like quarks, down-like quarks and charged

---

[7]In other words, SU(2) will only act on left-handed states
[8]The subscript L denotes the chirality on which this group acts

leptons respectively.

As doublets are the ones interacting via weak processes, a global $SU(2)_L$ transformation, for a general doublet ψ_L, takes the form [30]

$$\psi_L \to \exp\left(-ig_w\theta a\frac{\tau_a}{2}\right)\psi_L \quad \bar{\psi}_L \to \bar{\psi}_L \exp\left(ig_w\theta a\frac{\tau_a}{2}\right) \tag{2.42}$$

where $a = 1, 2, 3$, g_w is the weak coupling constant and τ_a are the Pauli matrices a. If the θ_a are space-time independent, the Lagrangian will be gauge invariant. Hence, by using Noether's theorem it is possible to obtain three conserved currents which are given by

$$J_a^\mu = g_w\bar{\psi}_L\gamma^\mu\frac{\tau_a}{2}\psi_L \tag{2.43}$$

To see the structure of these currents let us, without loss of generality, take ψ_L to be a lepton doublet, such that

$$J_1^\mu = \frac{g_w}{2}(\bar{\nu}_{eL}\gamma^\mu e_L + \bar{e}_L\gamma^\mu\nu_{eL}) \tag{2.44}$$

$$J_2^\mu = -i\frac{g_w}{2}(\bar{\nu}_{eL}\gamma^\mu e_L - \bar{e}_L\gamma^\mu\nu_{eL}) \tag{2.45}$$

$$J_3^\mu = \frac{g_w}{2}(\bar{\nu}_{eL}\gamma^\mu\nu_{eL} - \bar{e}_L\gamma^\mu e_L) \tag{2.46}$$

Note that J_3 takes a very familiar form, namely that of a neutral current like the one we obtained from QED [9]:

$$J_{EM}^\mu = Q\bar{e}\gamma^\mu e \tag{2.47}$$

Now that a theory which is globally invariant is obtained, this allows to consider local gauge transformations. I.e the fields map to

$$\psi_L \to \exp(-ig_w\theta a(x)T_a)\psi_L \quad \bar{\psi}_L \to \bar{\psi}_L \exp(ig_w\theta a(x)T_a); \quad T_a = \frac{1}{2}\tau_a \tag{2.48}$$

Note that making θ_a to be space-time dependent will break gauge invariance as

$$\partial_\mu\psi_L \to -ig_w(\partial_\mu\theta_a)T_a e^{-ig_w\theta_a(x)T_a}\psi_L + e^{-ig_w\theta_a(x)T_a}\partial_\mu\psi_L$$

Thus, inspired by QED results, one introduces the SU(2)$_L$ covariant derivative

$$D_\mu = \partial_\mu + ig_w T_a W_a^\mu, \tag{2.49}$$

where the W_a are the three vector fields that mediate weak interactions. Additionally, these bosons

---

[9]This fact would inspire Weinberg, Glashow and Salam to think of electromagnetism as a consequence of another phenomenon.

transform as [14]

$$W_a^\mu \to W_a^\mu + \frac{1}{g_w}\partial^\mu\theta_a - \epsilon_{abc}W_b^\mu\theta_c(x), \qquad (2.50)$$

where there last term arises from the non abelian behavior of SU(2).

In a similar way as for gluons, one introduces the field strength tensor as

$$F_{\mu\nu}^a = \partial_\mu W_\nu^a - \partial_\nu W_\mu^a + g_w \sum_{b,c} \epsilon^{bcd} W_\mu^c W_\nu^d \qquad (2.51)$$

With this definition, the total $SU(2)_L$ gauge invariant Lagrangian is given by

$$\mathcal{L} = i\bar{\psi}_L\gamma^\mu D_\mu\psi_L - \frac{1}{4}F_{\mu\nu}^a F_a^{\mu\nu} \qquad (2.52)$$

Note that the kinetic term for the W bosons will introduce 4-point and 3-point diagrams like those given in Figures 2.10 and 2.11
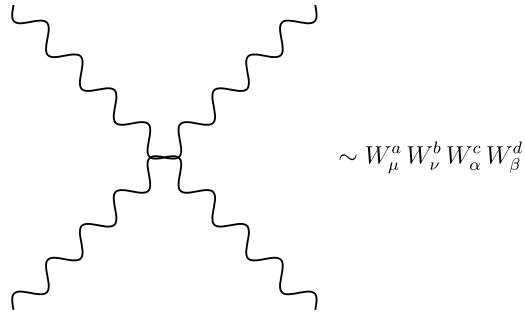

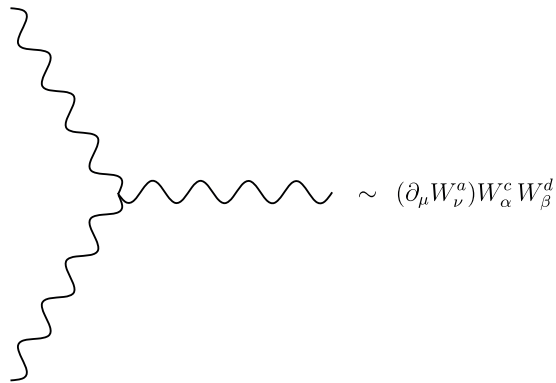Figure 2.10: 4-Point diagram arising from W boson Lagrangian

Figure 2.11: 3-Point diagram arising from W boson Lagrangian

As Equation 2.33 implies that T^2 and T_3 are diagonal, it is possible to define ladder operators

in analogy SU(2)-based spin in non relativistic quantum mechanics [10] [24, 27]

$$T_\pm = T_1 \pm iT_2 \tag{2.53}$$

This will then induce the construction of gauge bosons associated to these new degrees of freedom, namely [30]

$$W_\mu^\pm = \frac{1}{\sqrt{2}}(W_\mu^1 \mp iW_\mu^2), \tag{2.54}$$

as well as new charged currents given by

$$J_\pm^\mu = \frac{1}{2}(J_1^\mu \pm iJ_2^\mu) \tag{2.55}$$

Expanding for the lepton doublets, these currents take form [11] As a $SU(2)_L$ invariant Lagrangian was obtained, one could then try to get the Feynman rules at tree level for the weak interaction. However, the theory possess an additional symmetry which arises from the Dirac behavior of the spinors, just like they do in QED. In other words, by taking spinors to be Dirac-like one obtains an extra U(1) symmetry, referred as the hypercharge symmetry [12]

This new $U(1)_Y$ symmetry, when taken as global, maps the left-handed and right-handed states via Equations 2.56 and 2.57

$$\psi_L \to \exp\left(-\frac{i}{2}g'Y_L\theta\right)\psi_L \tag{2.56}$$

$$\psi_R \to \exp\left(\frac{i}{2}g'Y_R\theta\right)\psi_R \tag{2.57}$$

where g' is the $U(1)_Y$ coupling constant. Note that both left and right handed spinors are not forced to have the same hypercharge values, this is due to their doublet and singlet behavior under $SU(2)_L$. As the Lagrangian is gauge invariant under these new global transformations, one obtains two different Noether currents, one from each chirality, namely

$$J_\mu^{Y_L L/R} = \frac{g'}{2}Y_{L/R}\bar{\psi}_{L/R}\gamma^\mu\psi_{L/R}, \tag{2.58}$$

which for left-handed leptons becomes

$$J_\mu^{Y_L} = \frac{g'}{2}Y_L(\bar{\nu}_L\gamma_\mu\nu_L + \bar{e}_L\gamma_\mu e_L) \tag{2.59}$$

Following the same procedure as in QED it is possible to find that the derivative term breaks gauge invariance under local transformations, such that the introduction of two covariant derivatives (one

---

[10]This is also known as the spherical basis of SU(2)

[11]Experiments have shown that these linear combinations are the physical currents and gauge bosons.

[12]Thus, one adds a subscript Y to the U(1) group to distinguish from QED.

for each chirality) is needed

$$D_\mu^{L/R} = \partial_\mu + ig'Y_{L/R}B_\mu, \tag{2.60}$$

such that the gauge field B_μ transforms just like in Equation 2.12 as $U(1)_Y$ is abelian[13] The presence of the new $U(1)_Y$ gauge symmetry, together with $SU(2)_L$, in the weak interaction means that the total gauge group is $SU(2)_L \times U(1)_Y$. By acting simultaneously with both transformations, one obtains that the interacting Lagrangian is given by [42][14]

$$\mathcal{L} \supset -J_\mu^{Y_R}B^\mu - J_\mu^{Y_L}B^\mu - J_3^\mu W_\mu^3 - J_+^\mu W_\mu^+ - J_-^\mu W_\mu^- \tag{2.61}$$

For left-handed leptons, the neutral part of the Lagrangian reads

$$\mathcal{L} \supset \frac{-1}{2}[(g'Y_L B^\mu + g_w W_3^\mu)\bar{\nu}_L\gamma^\mu\nu_L + (g'Y_L B^\mu - g_w W_3^\mu)\bar{e}_L\gamma_\mu e_L] \tag{2.62}$$

This inspired Steven Weinberg, Glashow and Salam to realize that the B and W_3 fields were not the physical fields, but rather a superposition of them. Weinberg noticed that the structure of the interaction take a form similar to that of QED, namely $QA^\mu J_\mu$, inspiring his colleagues to confirm that the electromagnetic interaction, as well as the weak interaction, arise from a unified electroweak interaction. Additionally, he noticed that the matrix that takes the gauge fields to the physical fields must be a rotation to preserve unitarity in the weak interaction. Weinberg's rotation matrix is defined by

$$\begin{pmatrix} B^\mu \\ W_3^\mu \end{pmatrix} = \begin{pmatrix} \cos\theta_w & \sin\theta_w \\ -\sin\theta_w & \cos\theta_w \end{pmatrix} \begin{pmatrix} A^\mu \\ Z^\mu \end{pmatrix}, \tag{2.63}$$

where Z^μ is a new vector boson that mediates neutral currents and A^μ is the photon field. The weak mixing angle or Weinberg angle is then defined by [15]

$$-\frac{g'}{g_w} = \tan\theta_w \tag{2.64}$$

If one now replaces Equation 2.63 into 2.62, the neutral interaction Lagrangian will read

$$\begin{aligned}
\mathcal{L} \supset &-\left[Y_L\frac{g'}{2}\cos\theta_w - \frac{g_w}{2}\sin\theta_w\right]\bar{\nu}_L\gamma^\mu\nu_L A^\mu - \left[Y_L\frac{g'}{2}\cos\theta_w + \frac{g_w}{2}\sin\theta_w\right]\bar{e}_L\gamma^\mu e_L A_\mu \\
&-\left[Y_L\frac{g'}{2}\sin\theta_w + \frac{g_w}{2}\cos\theta_w\right]\bar{\nu}_L\gamma^\mu\nu_L Z_\mu - \left[Y_L\frac{g'}{2}\sin\theta_w - \frac{g_w}{2}\cos\theta_w\right]\bar{e}_L\gamma^\mu e_L Z_\mu
\end{aligned} \tag{2.65}$$

From the currents coupled to the photon, it is straightforward to show that the electric charge can

---

[13]From now on this document will only focus in the interacting part of the Lagrangian.

[14]The $\supset$ indicates that the terms on the right-hand side are part of the total Lagrangian.

[15]Experimental measurements have shown that $\sin^2\theta_w = 0.231$ [46]

be written in terms of the weak coupling constants as

$$Q = Y_L \frac{g'}{2} \cos \theta_w + \frac{g_w}{2} \sin \theta_w \tag{2.66}$$

As neutrinos are postulated as neutral particles, its coupling with the photon must vanish. This means

$$Y_L \frac{g'}{2} \cos \theta_w = \frac{g_w}{2} \sin \theta_w, \tag{2.67}$$

which reduces to $Y_L = -1$ after using Equation 2.64[16]. Additionally, note that $Y_L = -1$ along with Equation 2.64 imply that $Q = g_w \sin \theta_w$.

After replacing the electric charge and the hypercharge the neutral Lagrangian becomes

$$\mathcal{L} = -Q \bar{e}_L \gamma^\mu e_L A_\mu - \frac{g_w}{2 \cos \theta_w} \bar{\nu}_L \gamma^\mu \nu_L Z_\mu + \frac{g_w}{2 \cos \theta_w} \cos(2\theta_w) \bar{e}_L \gamma^\mu e_L Z_\mu \tag{2.68}$$

When reading this Lagrangian, one notes that that neutrinos and leptons behave differently when interacting with the Z boson. This fact was indeed seen at experiments such as LEP [47] and TEVATRON [48], where the branching fraction of the Z boson to leptons and neutrinos are approximately 10% and 20% respectively [46]. Furthermore, note that the definition of the electric charge in terms of both hypercharge and couplings to the W_3 boson imply that the Gell-Mann-Nishijima formula holds in the electroweak interaction due to the $SU(2) \otimes U(1)$ structure of the gauge group, namely

$$Q = T_3 + \frac{1}{2} Y_{L/R}$$

If one now follows the same procedure with the right-handed states, it can be found that $Y_R(\nu_R) = 0$, $Y_R(e_R) = -2$, $Y_R(u_R) = \frac{4}{3}$ and $Y_R(d_R) = -\frac{2}{3}$. Using Gell-Mann-Nishijima formula, one rewrites the Z boson Lagrangian, for a generic spinor ψ, as

$$\mathcal{L} \supset \frac{-g_w}{2 \cos \theta_w} [T_3 - Q \sin^2 \theta_w] \bar{\psi} \gamma^\mu \psi Z_\mu \tag{2.69}$$

As the Z boson is a superposition of both B and W_3, it couples differently to each component of the (V-A) currents that participate in the weak interaction, namely

$$\mathcal{L} = -\frac{g_w}{2 \cos \theta_w} \bar{\psi} \gamma^\mu (c_v - c_a \gamma_5) \psi Z_\mu, \tag{2.70}$$

where $c_v = T_{3L} - Q \sin^2 \theta_w$ and $c_a = T_{3L}$. Hence, the total Lagrangian, up to ghost field terms,
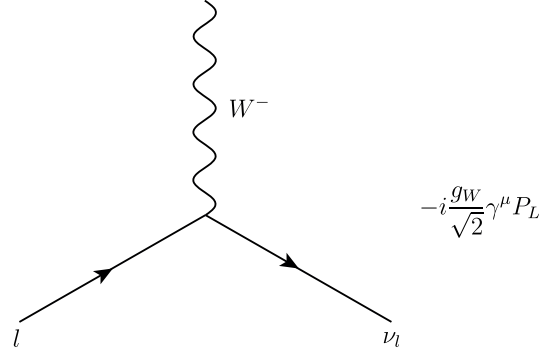
---

[16]This value only holds for leptons. For quarks one obtains $Y_L(u) = \frac{1}{3}$ and $Y_L(d) = \frac{1}{3}$ [24]
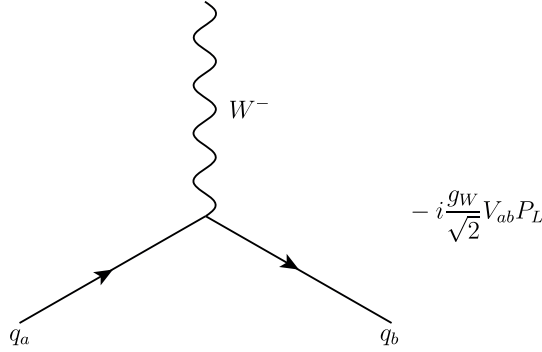
will now be

$$\mathcal{L} = i\psi\gamma^\mu\partial_\mu\psi - \frac{1}{4}F_{\mu\nu}F^{\mu\nu} - \frac{1}{4}Z_{\mu\nu}Z^{\mu\nu} - \frac{1}{4}W_{\mu\nu}W^{\mu\nu} - J^\mu_\pm W^\pm_\mu - Q\bar{\psi}\gamma^\mu\psi A_\mu - \frac{g_w}{2\cos\theta_w}\bar{\psi}\gamma^\mu(c_v - c_a\gamma_5)\psi Z_\mu,$$

$$(2.71)$$

such that one obtains the following Feynman rules

- Lepton-Neutrino coupling with W boson

$$-i\frac{g_W}{\sqrt{2}}\gamma^\mu P_L$$

- Quark coupling with W boson [17]

$$-i\frac{g_W}{\sqrt{2}}V_{ab}P_L$$

- Fermion coupling with the Z boson

$$-i\frac{g_W}{2\cos\theta_W}\gamma^\mu(C_v - C_a\gamma_5)$$

---
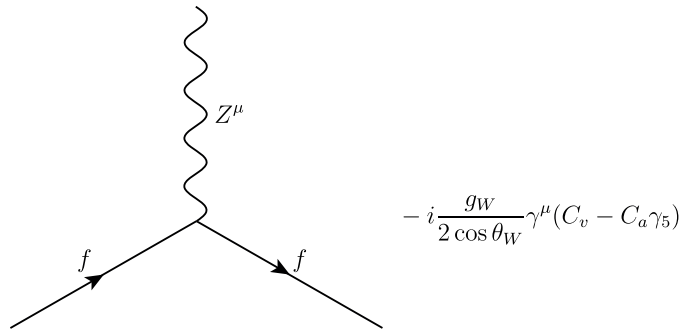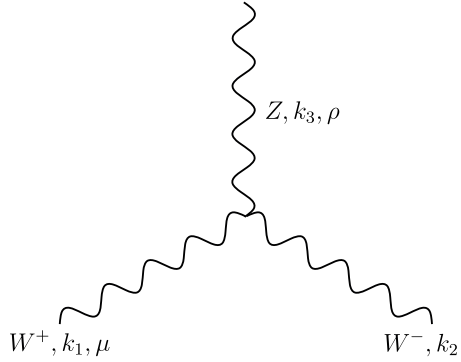
[17]Here the V_{ab} is the CKM quark mixing matrix, which arises from the experimental observation of CP violation in Kaon decay [27].

- Vector boson propagator
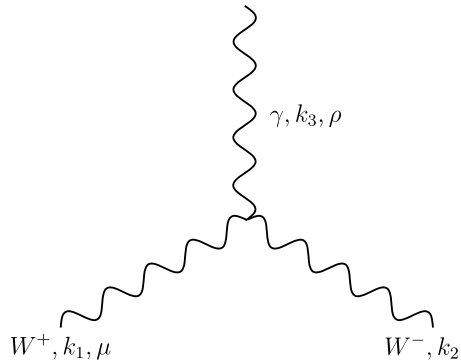
$$W^-/W^+/Z \qquad iD_{\mu\nu}(p) = -i\frac{(\eta_{\mu\nu} - p_\mu p_\nu/m^2)}{p^2 - m^2 + i\epsilon}$$

- W boson coupling with Z boson

Z, k_3, ρ

$$ig_W \cos\theta_W [\eta_{\mu\nu}(k_1 - k_2)_\rho + \eta_{\nu\rho}(k_2 - k_3)_\mu + \eta_{\rho\mu}(k_3 - k_1)_\nu]$$

W^+, k_1, μ $\qquad W^-, k_2, \nu$

- W boson coupling with the photon

γ, k_3, ρ

$$ig_W \sin\theta_W [\eta_{\mu\nu}(k_1 - k_2)_\rho + \eta_{\nu\rho}(k_2 - k_3)_\mu + \eta_{\rho\mu}(k_3 - k_1)_\nu]$$

W^+, k_1, μ $\qquad W^-, k_2, \nu$

- 4 vector boson coupling

W^-, ν $\qquad W^-, \rho$

$$ig_W^2 [2\eta_{\mu\delta}\eta_{\nu\rho} - \eta_{\mu\nu}\eta_{\delta\rho} - \eta_{\mu\rho}\eta_{\nu\delta}]$$

W^+, μ $\qquad W^+, \delta$

- W boson-Photon 4 point interaction

$$-ig_W^2 \sin^2\theta_W[2\eta_{\mu\nu}\eta_{\delta\rho} - \eta_{\mu\rho}\eta_{\nu\delta} - \eta_{\mu\delta}\eta_{\nu\rho}]$$

For the remaining Feynman rules see [24, 27, 30]

2.4   The Higgs Mechanism

In the last section a gauge invariant theory for fermions, interacting via weak processes, was found. However, one had to set vector boson and fermion masse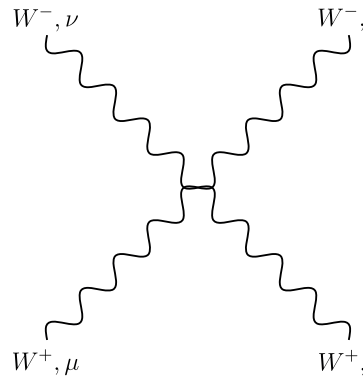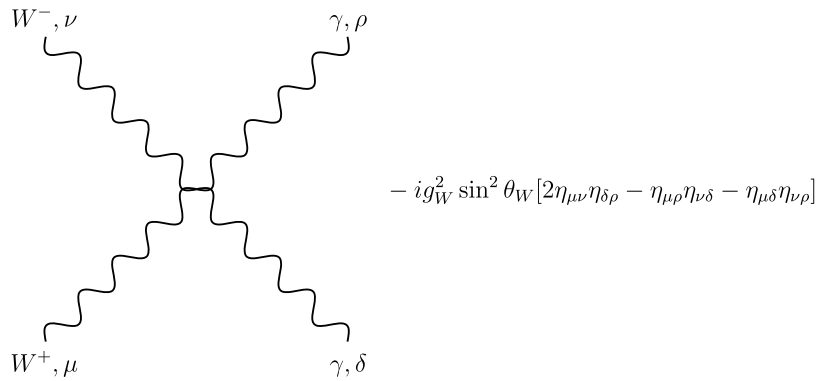s to zero in order to preserve guauge invariance under the electroweak gauge group. Setting masses to zero was a problem that needed a solution to give a proper prescription of the behavior of fermions.

The mass problem in the electroweak interaction was solved by Higgs, Englert, Kibble, Guralnik and other physicists after they analyzed how photons gain mass terms after Spontaneous Symmetry Breaking (SSB) in Ginzburg-Landau theory, giving rise to superconductivity and superfluidity. Based on this theory, they introduced a complex scalar doublet ϕ, whose dynamics are contained in the following Lagrangian [18]

$$\mathcal{L} = (\partial_\mu\phi)^*(\partial^\mu\phi) - V(\phi^*\phi) \tag{2.72}$$

where V is a self-interacting potential. n order to preserve gauge invariance and renormalizability, the potential must be given by [14]

$$V(\phi^*\phi) = \mu^2\phi^*\phi + \frac{\lambda}{4}(\phi^*\phi)2 \rightarrow \phi = \begin{pmatrix} \phi_1 \\ \phi_2 \end{pmatrix} \tag{2.73}$$

Note that if $\mu^2 > 0$ the potential will be symmetric, as seen in Figure 2.12, such that the minimum of the potential will be located at $\phi_0 = 0$.

---

[18]This doublet has $T_3 = \frac{1}{2}$ and Y=1
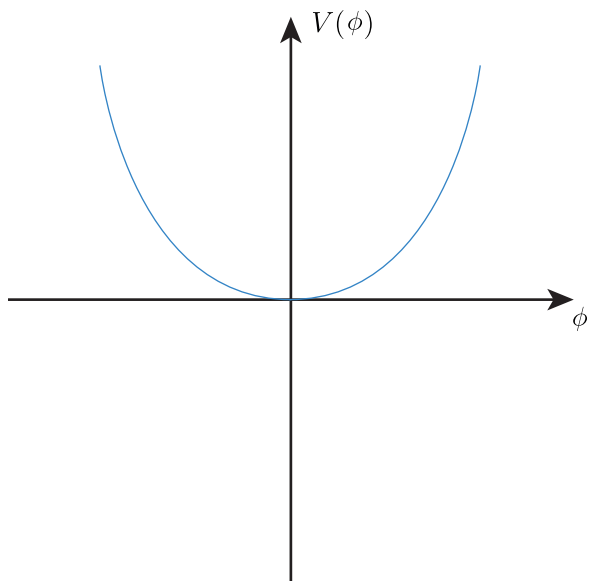
Figure 2.12: Interaction potential if $\mu^2 > 0$.

However, if μ^2 value becomes less than zero, for example due to a decreasing temperature, the symmetry of the potential due to this spontaneous change of sign [19] as seen in Figure 2.13
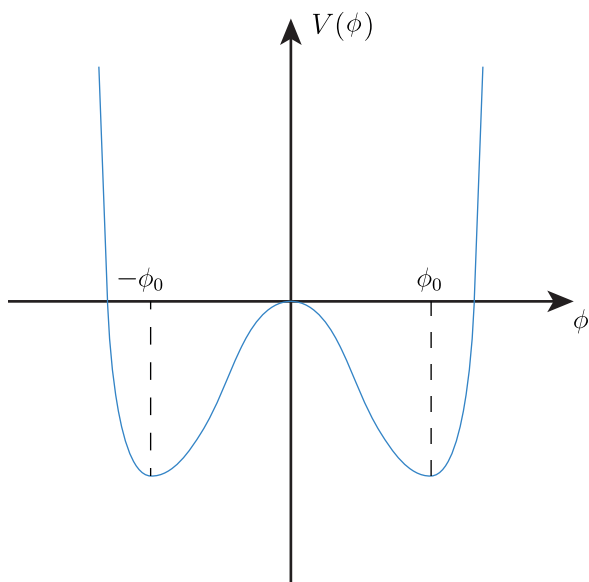
Figure 2.13: Interaction potential if $\mu^2 < 0$.

with minima occurring at $|\phi_0|^2 = \frac{-2\mu^2}{\lambda}$. Nevertheless, note that the minima are not unique and that a phase transition such as,

$$\phi_0 \rightarrow e^{-i\alpha}\phi_0 \tag{2.74}$$

will also be a minimum of the potential, leaving the dynamics of the field invariant. Thus, there is an infinite number of available minima, or vacuum expectation values, and that choosing one of

---

[19]That is why it is called an SSB. Note that it is also a phase transition.

them will break the symmetry of the potential.

Suppose now that nature chooses one of these minima, namely v. As the base of the potential is, topologically speaking, a circle no extra energy is required for moving around it, introducing redundancies known as Goldstone bosons [14] [20]. As choose of a minimum has been done, it is possible to expand the doublet in terms of angular and radial modes (Goldstone and Higgs fields respectively) as [21]

$$\phi = \begin{pmatrix} G^{\pm} \\ \frac{v+h+iG^0}{\sqrt{2}} \end{pmatrix} \tag{2.75}$$

To eliminate the presence of Goldstone modes one uses the so called *Unitary Gauge*, such that the doublet becomes [49]

$$\phi = \begin{pmatrix} 0 \\ \frac{v+h}{\sqrt{2}} \end{pmatrix} \tag{2.76}$$

To preserve the local $SU(2) \times U(1)$ gauge invariance of the doublet Lagrangian, one introduces the covariant derivative

$$D_\mu = \partial_\mu + ig_w T_a W_\mu^a + i\frac{g'}{2}B_\mu, \tag{2.77}$$

such that the gauge invariant Lagrangian is

$$\mathcal{L} = (D_\mu\phi)^*(D^\mu\phi) - \mu^2\phi^*\phi - \frac{\lambda}{4}(\phi^*\phi)^2 \tag{2.78}$$

Now, from this Lagrangian one can take the part that only considers vector bosons and no interactions with the Higgs field, h, reads [14]

$$(D_\mu\phi)^*(D^\mu\phi) \supset \left| \left(\partial_\mu + ig_w T_a W_\mu^a + i\frac{g'}{2}B_\mu \right) \times \frac{1}{\sqrt{2}}\begin{pmatrix} 0 \\ v \end{pmatrix} \right|^2 \tag{2.79}$$

$$= \frac{v^2}{8}\left| \left(g_w \tau_a W_\mu^a + g'B_\mu \mathbb{1} \right)\begin{pmatrix} 0 \\ 1 \end{pmatrix} \right| \tag{2.80}$$

Expanding the sum over a in terms of the Pauli matrices one obtains

$$(D_\mu\phi)^*(D^\mu\phi) \supset \frac{v^2}{8}\left| \begin{pmatrix} g_w W_1^\mu - ig_w W_2^\mu \\ -g_w W_3^\mu + g'B^\mu \end{pmatrix} \right|^2 \tag{2.81}$$

$$= \frac{v^2}{8}[g^2(W_1^\mu W_\mu^1 + W_2^\mu W_\mu^2) + (g_w W_3^\mu - g'B^\mu)^2] \tag{2.82}$$

---

[20]Formally speaking, Goldstone bosons are redundant degrees of freedom in a local gauge theory, whereas they become relevant at global symmetry breaking of gauge theories.

[21]This parametrization is known as Higgs-Kibble or Kibble parametrization.

By replacing the W bosons in terms of the $\pm$ fields, as well as W_3 and B in terms of Equation 2.63, the Lagrangian becomes

$$(D_\mu\phi)^*(D^\mu\phi) \supset \frac{1}{2}\left(\frac{g_w v}{2}\right)^2 W_\mu W^\mu + \frac{1}{2}\frac{v^2(g_w^2 + g'^2)}{4}Z_\mu Z^\mu \tag{2.83}$$

$$= \frac{1}{2}m_w^2 W_\mu W^\mu + \frac{1}{2}m_z^2 Z_\mu Z^\mu \tag{2.84}$$

This result is one of the most important in physics as it explains how gauge bosons gain mass due to SSB, thus explaining why the weak interaction is short ranged. Note that there is no mass term for photons, as the terms related to its linear combination cancel out.

To explain fermion masses one then considers Yukawa couplings with the Higgs field [34]

$$\mathcal{L}_{Yuk} = \Gamma_{ij}^u \bar{q}_{Li}\tilde{\phi}u_{Rj} + \Gamma_{ij}^d \bar{q}_{Li}\phi d_{Rj} + \Gamma_{ij}^e \bar{e}_{Li}\phi e_{Rj}; \quad \tilde{\phi} = i\tau_2\phi^*, \tag{2.85}$$

where the Γ matrices are the couplings between fermions and the Higgs doublet (or its conjugated version $\tilde{\phi}$). Note that the Yukawa couplings to be between left-handed and right-handed states have been conveniently constructed, as mass terms arise as a direct coupling between them according to Equation 2.39.

For simplicity, and without loss of generality, consider only one lepton family. Now, if ϕ gets a vacuum expectation value, it is parametrize it using Equation 2.75, such that the Lagrangian reads

$$\mathcal{L} \supset f_e \bar{e}_L\left(\frac{v+h}{\sqrt{2}}\right)e_R \tag{2.86}$$

$$= \frac{f_e v}{\sqrt{2}}\bar{e}_L e_R + \frac{f_e}{\sqrt{2}}\bar{e}_L h e_R \tag{2.87}$$

Hence, one defines the lepton mass as $m_e = \frac{f_e v}{\sqrt{2}}$. With this definition, the Lagrangian becomes

$$\mathcal{L} \supset m\bar{e}_L e_R + \frac{m}{v}\bar{e}_L h e_R \tag{2.88}$$

recovering fermion masses within the formalism.

So, mass terms for fermions, based on SSB and couplings with the Higgs boson, have been obtained . This being said, one can write a total gauge group for the strong and electroweak interactions, without unifying them yet. To see this recall that quarks interact under the SI and also under the electroweak interaction, acting as color triplets, left-handed doublets and right-handed singlets respectively. Thus, one can say that a total gauge theory for quarks is invariant under the gauge group given in Equation 1.2

Additionally, this group also describes a gauge theory of leptons as experiments have shown that leptons do not participate in the SI, therefore they are considered color singlets. Hence, note that a local Lorentz invariant gauge theory that describes three of the fundamental forces of nature has been obtained.

3. State of The Art

The SM, together with General Relativity (GR), is one of the most precise theories in physics, as it describes the electromagnetic coupling constant g_e with 12 significative figures of precision [46]. The SM is describes how the electromagnetic, weak, and strong interactions among fermions are mediated by spin-1 bosons. In addition to this, the SM gives mass terms to all particles, except neutrinos, via Spontaneous Symmetry Breaking (SSB) of the electroweak gauge group $SU(2) \times U(1)$.

Nevertheless, the SM is an incomplete theory as it cannot describe many experimental and phenomenological aspects, such as quantum triviality, Higgs boson mass finiteness, matter-Antimatter asymmetry, neutrino oscillations-mass, quantum gravity

Thus, the SM has to be expanded into a more complete theory. According to the SM, neutrinos are massless particles which only interact via weak interactions [30]. Being massless particles, neutrinos can be introduced in the SM as part of a left-handed $SU(2)_L$ doublet, together with the left-handed component of its associated charged lepton

$$\begin{pmatrix} \nu_\ell \\ \ell \end{pmatrix}_L$$

whereas the right-handed component of the charged lepton is introduced as a singlet ℓ_R. However, experimental analysis of solar neutrinos show that they oscillate between flavor states, when travelling a distance L, which can only be explained if neutrinos have mass. Then, the transition probability between two flavors, as a function of L, is given by [50]

$$P(L) = \sin^2(2\theta) \sin^2 \left[\frac{1.27 \Delta m^2 L}{E} \right], \tag{3.1}$$

where θ is the mixing angle between the two flavors, and Δm^2 is the difference of the square masses of the neutrinos, which according to experiments is very small [51]. On this work, we will focus on the neutrino mass problem, giving priority to the lepton sector of the weak interaction.

As the introduction of mass to neutrinos explains the oscillation between flavor states, there should be neutrino mass terms in the SM-Lagrangian, which are not present. To include these terms, one has to consider the introduction of right-handed singlets, ν_R, that should interact with the SM Higgs to produce mass terms of the SM neutrinos. This means that we have to introduce a Yukawa coupling between the Higgs, and our new neutrino states:

$$-\mathcal{L}_m \supset f_{ij}^\nu \bar{\ell}_L^i \tilde{\phi} \nu_R^j \tag{3.2}$$

In Equation 3.2 f_{ij}^ν are the Yukawa couplings to neutrinos, ℓ is the lepton doublet, ν_R is the right-handed neutrino component, and $\tilde{\phi}$ is the charge conjugated Higgs field, which defined as $\tilde{\phi} = i\tau_2 \phi$.

Now, to produce mass terms, we have to consider SSB of the SM gauge group, this can be done by introducing the Kibble parametrization of the Higgs field

$$\phi = \frac{1}{\sqrt{2}} \begin{pmatrix} 0 \\ v+h \end{pmatrix}, \tag{3.3}$$

that leads to

$$-\mathcal{L}_m \supset \frac{1}{\sqrt{2}} f_{ij}^\nu \bar{\ell}_L^i \nu_R^j v + \frac{1}{\sqrt{2}} f_{ij}^\nu \bar{\ell}_L^i \nu_R^j h \tag{3.4}$$

Now, only focusing on the neutrino sector, i.e $\ell_i = \nu_i$, and if we follow the usual SM SSB, the Dirac mass matrix can be defined as $(M_D)_{ij} = \frac{1}{\sqrt{2}} f_{ij}^\nu v$. This definition allows us to reduce the Lagrangian to

$$-\mathcal{L}_m = (M_D)_{ij}^\nu \bar{\nu}_L^i \nu_R^j + \frac{1}{\sqrt{2}} f_{ij}^\nu \bar{\nu}_L^i \nu_R^j h + h.c \tag{3.5}$$

Note that the second term can be understood in terms of the Feynman diagram in Figure 3.1
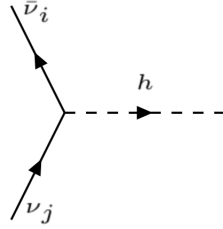
Figure 3.1: Feynman diagram associated to a $\bar{\nu}\nu h$ coupling

Even though Equation 3.5 explains how the measured neutrino masses are generated by the introduction of new right-handed states, it does not explain the smallness of these masses. To do so, we will follow [50, 52, 53] and introduce an arbitrary number, n_i, of massive Majorana neutrinos. The Lagrangian describing the mass term of Majorana neutrinos is

$$-\mathcal{L}_M = \frac{1}{2} \bar{\nu}_L^c M_M \nu_R + h.c, \tag{3.6}$$

where we introduced the charged conjugated field $\nu_L^c = C\bar{\nu}_L^T$. Then, to make a more profound study of the origins of neutrino masses, it is natural to consider the complete neutrino mass Lagrangian, which contains the Majorana and Dirac terms:

$$-\mathcal{L}_m \supset \frac{1}{2}[\bar{\nu}_L M_D \nu_R + \bar{\nu}_L^c M_D^T \nu_R^c + \bar{\nu}_L^c M_M \nu_R] + h.c \tag{3.7}$$

$$= \frac{1}{2} \bar{\nu}_L M_N \nu_R + h.c \tag{3.8}$$

In the previous equation we have redefined the neutrino states and the mass matrix as

$$\nu_R = (\nu_L^c, \nu_R)^T; \; M_N = \begin{pmatrix} 0 & M_D \\ M_D^T & M_M \end{pmatrix}$$

Now, note that the mass matrix M_N is non diagonal. This means that the weak interaction eigenstates do not correspond with the mass eigenstates. Therefore, we have to diagonalize the mass matrix. This can be done by means of an orthogonal transformation V, such that we obtain a diagonal matrix [54, 55]

$$M_d = \text{diag}(m_1, m_2, \cdots, m_i) = V^T M_N V, \tag{3.9}$$

where the m_i are the eigenvalues of the mass matrix. After diagonalization, we obtain M_d from the decomposition of M_N in it's two possible eigenmatrices

$$M_N' = \text{diag}(\lambda_+, \lambda_-); \lambda_\pm = \frac{1}{2}[M_M \pm \sqrt{M_m^2 + 4M_D^T M_D}] \tag{3.10}$$

One interesting scenario, and one of the main focuses of this project, is the so called Seesaw mechanism. In the Seesaw scenario, it is assumed $M_M \gg M_D$. In other words, we set the masses of the right-handed Majorana neutrinos to be bigger than those of the SM-neutrinos. This allows us to expand the squared root and rewrite both eigenmatrices as:

$$\lambda_\pm = \frac{1}{2}[M_M \pm M_M(\mathbb{1} + 2(M_M^{-1})^2 M_D^T M_D)] \tag{3.11}$$

This reduces M_N' to

$$M_N' = \begin{pmatrix} M_M & 0 \\ 0 & -M_M^{-1} M_D^T M_D \end{pmatrix} \tag{3.12}$$

To better illustrate this idea, let us consider just one neutrino flavor. Then, the mass eigenmatrices reduce to single eigenvalues:

$$\lambda_\pm = \frac{1}{2}\left[m_m \pm m_m \left(1 - 2\frac{m_D^2}{m_m^2}\right)\right]$$

$$\lambda_+ = m_m; \quad \lambda_- = \frac{m_D^2}{m_m}$$

Note that for the second mass eigenvalue, we have that it will be very small if the newly introduced Majorana neutrino is very heavy. So, it is possible to associate λ_- with the SM-neutrinos.

Even though the introduction of very heavy Majorana neutrinos solves the mass problems via Seesaw, it introduces one deep problem as the lepton number, L, is not preserved in any process involving them. As a matter of fact, the mass term of Majorana neutrinos breaks L by two units, creating a lepton excess. Nonetheless, these excess can be used to explain the observed asymmetry

between matter-antimatter in the universe, namely via Leptogenesis [12].

In the SM, both baryon number (B) and L are not explicit symmetries of the model, but the arise as one via perturbative analysis. In other words, B and L become symmetries by analyzing how they behave at any order of the S matrix. Being L one of the symmetries of the SM, we shall now explore a way to break it; to do so we promote L (or B-L) to be a U(1) gauge symmetry of the SM, this extends the electroweak gauge group to

$$G_{EW} = SU(2)_L \times U(1)_Y \times U(1)_{L/B-L} \tag{3.13}$$

In this project we will focus on a global breaking of the $U(1)_{L/B-L}$ gauge group via a scalar singlet φ. However, many authors such as [56, 57] have studied the consequences of a local breaking of this symmetry, which introduces a new vector boson, the Z' boson. The introduction of this new scalar singlet allows us to expand the Higgs sector to [58]

$$-\mathcal{L} = m_\phi^2 \phi^\dagger \phi + \frac{\lambda_\phi}{2}(\phi^\dagger \phi)^2 + m_\varphi^2 \varphi^\dagger \varphi + \frac{\lambda_\varphi}{2}(\varphi^\dagger \varphi)^2 - V(\phi, \varphi) \tag{3.14}$$

Here we just focus on the expansion of the Higgs sector by a singlet scalar charged under $U(1)_{B/B-L}$, this means that the potential V can be ignored as it is meaningless in our study. However, some authors such as [58], consider a mixing potential between the SM Higgs doublet and the singlet. After defining our Higgs extension, we now consider a Kibble parametrization for both the singlet and doublet as:

$$\phi = \begin{pmatrix} G^+ \\ \frac{v+h+G^0}{\sqrt{2}} \end{pmatrix}; \quad \varphi = \frac{1}{\sqrt{2}}(f + A + iJ) \tag{3.15}$$

Note that we have in total four Goldstone modes; three of them $(G^0, G^\pm)$ get eaten by the W and Z bosons, giving them longitudinal polarization modes, while one of them, J, remains free in the model. We will now refer to J as the Majoron, and we will consider it to be massive [54, 55, 59].

Note that we now require an extension of the Yukawa sector, we do this by inserting new couplings between $U(1)_{L/B-L}$ charged particles, namely between the Heavy Neutrino eigenstates (HN) and the scalar singlet:

$$-\mathcal{L}_{Yuk} \supset \frac{1}{2} y_{ij} \bar{\nu}_L^{c,i} \varphi \nu_R^j \tag{3.16}$$

After SSB of the L symmetry, Majorana mass terms are generated as well as couplings between the HN with A and the Majoron:

$$-\mathcal{L}_{Yuk} \supset \frac{1}{2} M_{M,ij} \bar{\nu}_L^{c,i} \nu_R^j + \frac{1}{2\sqrt{2}} y_{ij} \bar{\nu}_L^{c,i} A \nu_R^j + \frac{i}{2\sqrt{2}} y_{ij} \bar{\nu}_L^{c,i} J \nu_R^j; \tag{3.17}$$

Note that we found a way of generating L-breaking Majorana masses for the right-handed neutrinos, and generated neutrino mixing. Now, after changing to the neutrino mass eigenstates,n_i, we follow

[55] for the tree-level Lagrangian J-HN coupling (also after SM unitary gauge):

$$-\mathcal{L}_{JN} = \frac{i}{2f} \sum_{i,j=1}^{6} \bar{n}_i [C_{ij}(m_i P_L - m_j P_R) + C_{ji}(m_j P_L - m_i P_R) + \delta_{ij}\gamma^5 m_i] n_j J \tag{3.18}$$

Here, the C matrix is a 6×6 matrix related to the change of basis matrix V by

$$C_{ij} = \sum_{l=1}^{3} V_{li} V_{lj}^*$$

where the V matrix is related to the Pontecorvo-Maki-Nakagawa-Sakata (PMNS) neutrino mixing matrix, U, via [55]

$$C = \begin{pmatrix} \mathbb{1} - AA^\dagger & A \\ A^\dagger & A^\dagger A \end{pmatrix}; \quad A = U^\dagger M_D M_M^{-1}. \tag{3.19}$$

The consideration of neutrino mass eigenstates induces a neutrino-lepton mixing in the W boson Lagrangian, which is now given by [55]

$$\mathcal{L}_w \supset \frac{g_w}{\sqrt{2}} \sum_{i=1}^{6} \sum_{a=1}^{3} (\bar{\ell}_a B_{ai} \gamma^\mu W_\mu^- P_L n_i + \bar{n}_i B_{ai}^* \gamma^\mu W_\mu^+ P_L \ell_a) \tag{3.20}$$

Here B is the 3×6 neutrino lepton mixing matrix, which is related to the PMNS matrix via

$$B = \left(U\left(\mathbb{1} - \tfrac{1}{2}AA^\dagger\right) UA \right) \tag{3.21}$$

Given that the PMNS matrix has the values given in Equation 3.22 [46], it is straightforward to check that the lepton-neutrino mixing values are considerably small.

$$|U| = \begin{pmatrix} 0.799\cdots 0.844 & 0.516\cdots 0.582 & 0.141\cdots 0.156 \\ 0.242\cdots 0.494 & 0.467\cdots 0.678 & 0.639\cdots 0.774 \\ 0.284\cdots 0.521 & 0.490\cdots 0.695 & 0.615\cdots 0.754 \end{pmatrix} \tag{3.22}$$

Note it is possible to reduce the terms in the Lagrangian given in Equation 3.18, if we consider the Seesaw mechanism. This means that there are three negligible mass values, associated to the SM neutrinos. Additionally, this implies that the first two terms of the Lagrangian can be ignored, this leaves us with the reduced Lagrangian

$$-\mathcal{L}_{JN} = \frac{i}{2f} \sum_{i=1}^{3} m_i \bar{n}_i \gamma^5 n_i \tag{3.23}$$

these couplings can be represented on a Feynman diagram as seen in Figure 3.2. In this case, the

vertex factor for one neutrino is given by
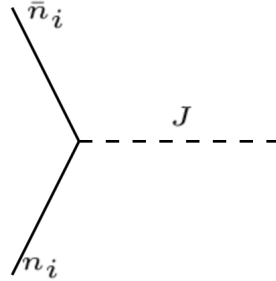
$$F_{vertex} = \frac{im}{2f}\gamma^5 \tag{3.24}$$

Figure 3.2: Feynman diagram of the J-HN coupling at tree level. Fermion flux has been ignored as the n_i are Majorana-like.

4. Production Mechanisms at the LHC.

In recent years the HN production mechanisms have been considered of great interest, as these particles can be consider DM candidates. However, no signal of these neutrinos has been found at the LHC experiments or any other experiment until now. Thus, the study of J-HN couplings arises as one possible scenario for DM production, as finding a Majoron can be an indirect signal for HN. Throughout this whole project we consider the J boson to be massive and stable, which simplifies some of the calculations without loss of generality.

In this project we will consider three possible production mechanisms that have been pillars of heavy particle production at the CERN's Large Hadron Collider(LHC). The first of them is known as the Drell-Yan Mechanism (DY) and allows us to study how particles couple to the color sector of a given theory [60]. The second production mechanism, VBF [61], allows to study production of new particles through electroweak-meadiated interactions [62, 63]. Nevertheless, we consider an indirect VBF production for the Majoron, such that it emulates its production to neutrinoless double beta decay [64]. Representative Feynman diagrams for the DY and VBF production mechanisms are presented in Figures 4.1 and 4.2, where fermion flux arrows have been placed for a better understanding of the Majorana behavior of HN.
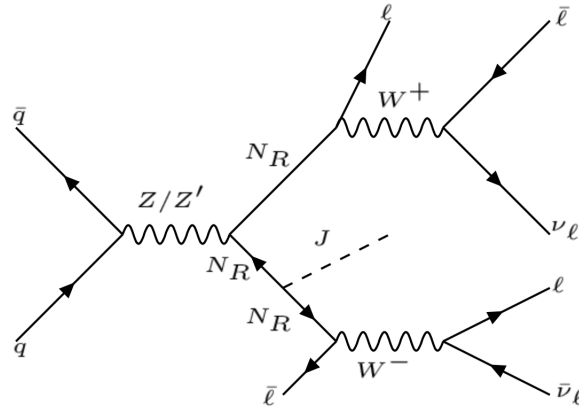
Figure 4.1: DY production mechanism of J via HN coupling.
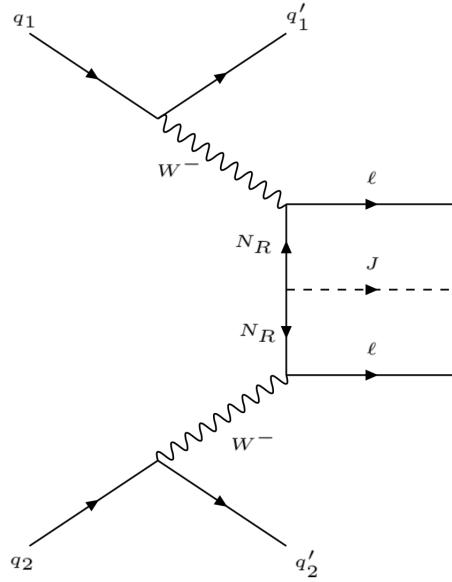
Figure 4.2: VBF production of J.

The third production mechanism that is being considered is J production via W boson exchange, or W channel, between a quark and antiquark pair and, together with the DY process, helps us to understand the coupling between the Majoron and the weak gauge bosons at tree level. The Feynman diagram of this process can be seen in Figure 4.3 [65]

Figure 4.3: Tree-level production of a J via W channel

5. Experimental Setup

The simulations were performed based upon the CMS input card in Delphes. Therefore, a brief introduction to the detector and its experimental parameters is presented, in order to understand the feasibility study associated to this dissertation.
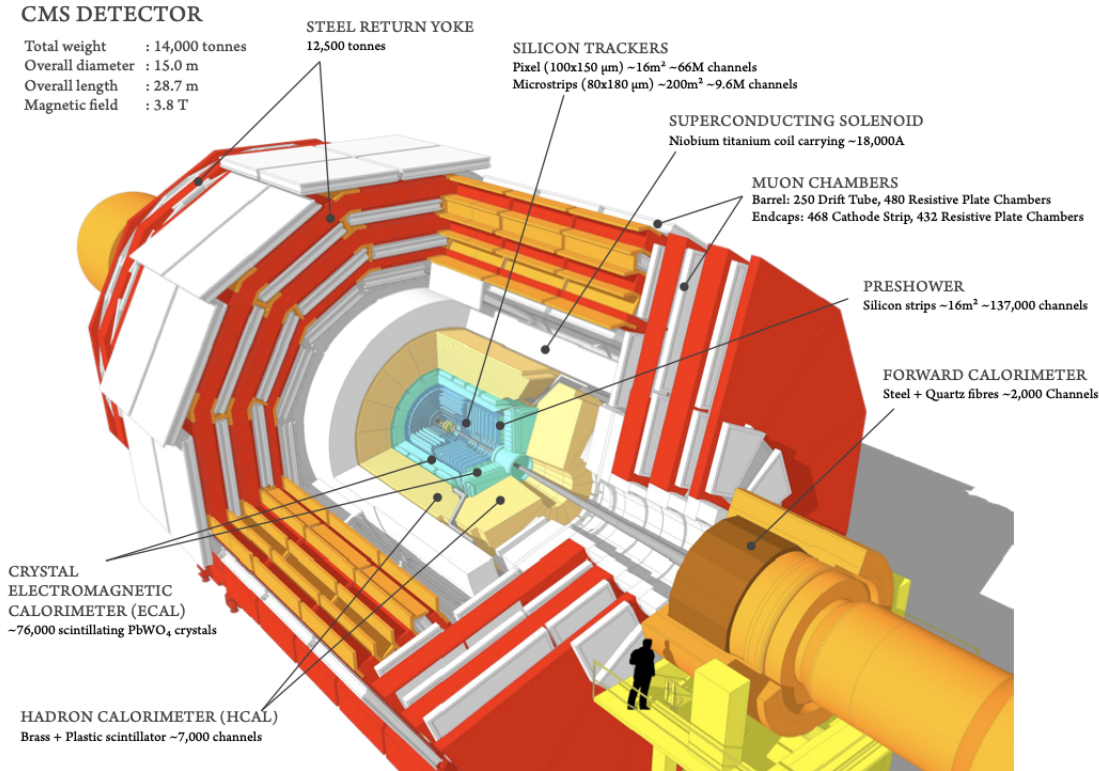
Figure 5.1: Sketch of the CMS detector components. Adapted from [66]

The CMS experiment is a multi-purpose detector at CERN's LHC. It has a length of 21.6 meters, with a diameter of 14.6 meters and weights 12500 tonnes. The detector is composed of a set of different sub-detecto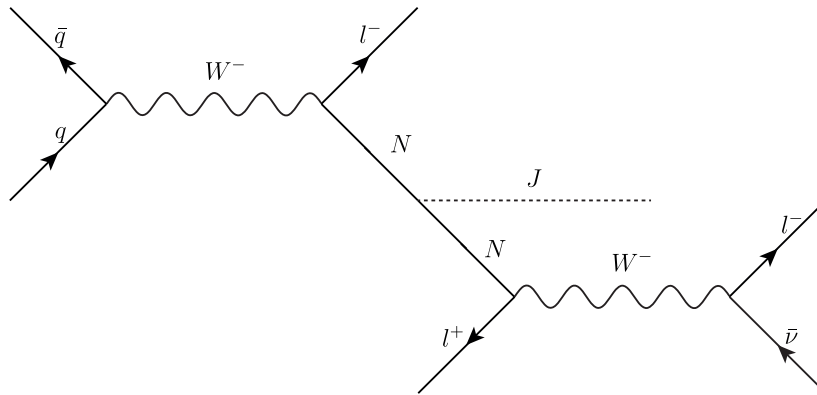rs as seen in Figure 5.1. The CMS detector has a cylindrical shape and it is divided into two main sections: barrel and endcaps. The different sub-detectors are located concentrically in layers [16]. The inner most layer has a pixel detector made out of silicon, used for the reconstruction of primary and secondary vertices from electrically charged particles that decay promptly within this sub-detector volume. The pixel detector is followed by a sub-detector made of silicon strips, known as the tracker detector, used for the reconstruction of trajectories of electrically charged particles. Following the tracker detector, are found the electromagnetic (ECAL) and hadron (HCAL) calorimeters, used to measure both energy and direction of the particles undergoing electromagnetic and strong interactions, respectively. The ECAL detector is a modular device composed of lead-tugsten crystals, highly efficient to produce electromagnetic showers after interacting with charged particles. The emerging photons from the showers are measured using photo-diodes, that collect the light produced from the signal and convert it into

an electric signal. This signal is then used by software tools to detect the energy and direction of the corresponding particles [67]. The ECAL is made of non magnetic materials such as copper and steel, which are characterized by heavy nuclei favoring strong interactions. Following a similar functioning as ECAL, hadronic particles enter the calorimeter, interact with the non-magnetic layers producing hadronic showers. These showers are then detected by plastic scintillators and their signals are transformed into electric pulses. These signals are then analyzed to estimate the energy and direction of the original particles [16].

The next layer of the detector consists of a superconducting solenoid, which surrounds the previous sub-detectors. This solenoid is made of a niobum-titanium alloy that is refrigerated to 2K by using liquid helium, producing a uniform magnetic field of 3.8T inside the barrel [67]. This magnetic field is used to measure the momentum of electrically charged particles as it induces curvatures in their trajectories.

Finally, the last set sub-detectors conform the muon detector system. This system is made of three different detector technologies, that allow to reconstruct the trajectory of the muons with a fast trigger response, and are alternated with iron returning yokes of steel to enclose the magnetic field produced by the solenoid. The trigger is a date-filtering system composed of hardware and software algorithms, designed to collect interesting events from the proton-proton collisions. The muon detectors have a total of 1400 chambers distributed in 250 drift tubes, 540 cathode strip chambers that track the position of a muon and provide a trigger, as well as 610 resistive plate chambers that give a redundant trigger, which quickly decide over the event storage [68].

5.1 Experimental Parameters

Before defining the experimental parameters of the CMS detector, it is useful to consider its geometry, which is presented in Figure 5.2.
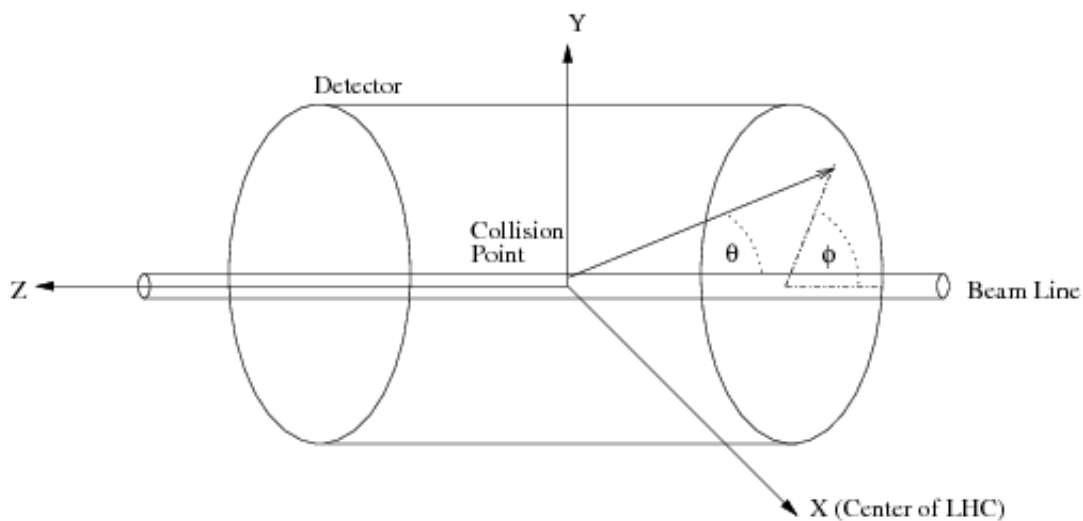

Figure 5.2: Coordinate system of the CMS detector. Adapted from [69]

- Luminosity ($\mathcal{L}$) The luminosity gives a measure of the performance of the accelerator. For

head on colliding Gaussian beams, such as the LHC ones, the luminosity is given by [70]

$$\mathcal{L} = \frac{N_1 N_2 f N_b}{4\pi\sigma_x\sigma_y}, \tag{5.1}$$

where N_1 and N_2 are the number of particles per bunch, f the revolution frequency, N_b the number of bunches per beam and the effective interaction area $4\pi\sigma_x\sigma_y$. However, if these collisions are not head on, such that the beams interact at a relative scattering angle α, the luminosity is given by

$$\mathcal{L} = \frac{N_1 N_2 f N_b}{4\pi\sigma_x\sigma_y}\alpha \tag{5.2}$$

For the LHC, it has been measured that $\mathcal{L} = 2.06 \times 10^{34} cm^{-2}s^{-1}$ [71]. Additionally, one can also consider the integrated luminosity, which is given by

$$L = \int_{t_1}^{t_2} dt\mathcal{L}, \tag{5.3}$$

as it is directly related to the interaction cross section and the total number of events via

$$L\sigma = N \tag{5.4}$$

- Cross Section (σ) The cross section, σ, is used in particle physics as a measure of the production probability of a certain process per unit area. This variable is related to the type of interaction between the colliding beams, the integrated luminosity of the collider and the total number of events.

- Missing Transverse Energy The Missing Transverse Energy (MET) or Missing Transverse Momentum, p_T^{miss}, is a measure of the energy associated to undetected particles such as neutrinos or even new physics. To take these particles into account, one considers total momentum conservation of both detected and undetected particles [72]

$$\sum_a \vec{p}_T^{\,a}(detected) + \sum_b \vec{p}_T^{\,b}(undetec) = 0 \tag{5.5}$$

$$\vec{p}_T^{\,miss} = -\sum_a \vec{p}_T^{\,a} \tag{5.6}$$

one then takes the magnitude of the vector given in the last equation to be the MET or p_T^{miss}.

- Pseudorapidity (η) The CMS detector does not use explicitly the polar angle θ. In its place the pseudorapidity η is used. As a major advantage comes that η gives a significantly more uniform distribution of the particle multiplicity across the detector volume than the θ angle. Additionally, the pseudorapidity difference between two particles is a Lorentz invariant quantity if a Lorentz transformation parallel to the beam line is performed. The definition

of η is given by [1]

$$\eta = -\ln\left(\tan\frac{\theta}{2}\right) \tag{5.7}$$

6. Calculation of the production matrix element of a Majoron via DY Mechanism.

For this calculation, as well as for further ones, we follow the standard electroweak Feynman rules given in [24] and choose Majorana fermion propagators given in [73].

After assigning momentum values to all particles we obtain the Feynman diagram that can be seen in Figure 6.1.
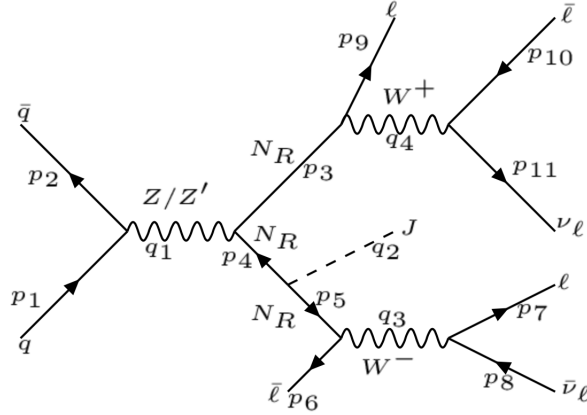
Figure 6.1: Feynman diagram of DY production of a J after momentum assignation.

Our first step is to find momentum conservation rules, these can be easily obtained from the Feynman diagram:

$$p_1 - p_2 = q_1 \tag{6.1}$$
$$p_3 - p_4 = q_1 \tag{6.2}$$
$$q_2 - p_4 = p_5 \tag{6.3}$$
$$p_5 - p_6 = q_3 \tag{6.4}$$
$$p_7 - p_8 = q_3 \tag{6.5}$$
$$p_3 + p_9 = q_4 \tag{6.6}$$
$$p_{11} - p_{10} = q_4 \tag{6.7}$$
$$\tag{6.8}$$

After a little algebra, all these momentum conservation relations can be reduced to

$$q_2 = p_1 + p_2 + p_7 + p_8 - p_6 - p_9 - p_{11} - p_{10} \tag{6.9}$$

This being established we can write the matrix element for the process

$$
i\mathcal{M} = [\bar{u}(p_{11}) \times \frac{-i\alpha_w}{\sqrt{2}}\gamma^\epsilon P_L \times v(10)] \times iD^W_{\eta\epsilon}(q_4) \times [\bar{u}(p_9) \times \frac{-i\alpha_w}{\sqrt{2}}\gamma^\eta P_L \times iS_F(p_3)]
$$

$$
\times [\bar{u}(p_7) \times \frac{-i\alpha_w}{\sqrt{2}}\gamma^\kappa P_L \times v(p_8)] \times iD^W_{\beta\kappa}(q_3) \times [\bar{v}(p_6) \times \frac{-i\alpha_w}{\sqrt{2}}\gamma^\beta P_L \times iS_F(p_5)]
$$

$$
\times iS_F(p_4)C \times \frac{im_N}{2f}\gamma^5 \times iD^Z_{\mu\nu}(q_1) \times \frac{-ig_z}{\sqrt{2}}\gamma^\nu(c^N_A - c^N_V\gamma^5) \times [\bar{v}(p_2)
$$

$$
\times \frac{-ig_z}{\sqrt{2}}\gamma^\mu(c^q_A - c^q_V\gamma^5) \times u(p_1)]
$$

(6.10)

where the left-handed projection operator is $P_L = \frac{1}{2}(1-\gamma^5)$. Due to the Majorana nature of N_R, we can get rid of the charge conjugation operator [74]:

$$
\bar{v}(p_6) \iff u(p_6)
$$

(6.11)

Now, let us analyze each current contained in the matrix element such that it takes the form

$$
-i\mathcal{M} = A \times B \times E \times D
$$

For the A term we have

$$
A = [\bar{u}(p_{11}) \times \frac{-i\alpha_w}{\sqrt{2}}\gamma^\epsilon P_L \times v(10)] \times iD^W_{\eta\epsilon}(q_4) \times [\bar{u}(p_9) \times \frac{-i\alpha_w}{\sqrt{2}}\gamma^\eta P_L \times iS_F(p_3)]
$$

(6.12)

$$
= \frac{-\alpha_w^2}{2}[\bar{u}(p_{11})\gamma^\epsilon P_L v(p_{10})] \times iD_{\epsilon\eta}(q_4)^W \times [\bar{u}(p_9)\gamma^\eta P_L iS_F(p_3)]
$$

(6.13)

Let us now rewrite A in terms of the propagator

$$
iD_{\mu\nu}(q) = i\Pi(q)\left(\eta_{\mu\nu} - \frac{q_\mu q_\nu}{m_W^2}\right); \quad \Pi(q) = \frac{1}{q^2 - m_W^2}
$$

(6.14)

Hence

$$
A = -\frac{-i\Pi(q_4)\alpha_w^2}{2}[\bar{u}(p_{11})\gamma^\epsilon P_L v(p_{10})](\eta_{\epsilon\eta} - q_{4\epsilon}q_{4\eta}/m_W^2)[\bar{u}(p_9)\gamma^\eta P_L iS_F(p_3)]
$$

(6.15)

After expanding the propagator terms, A takes the form

$$
A = -\frac{i\Pi(q_4)\alpha_w^2}{2}\left\{ [\bar{u}(p_{11})\gamma_\eta P_L v(p_{10})][\bar{u}(p_9)\gamma^\eta P_L iS_F(p_3)] \cdots \right.
$$

$$
\left. \cdots - \frac{1}{m_W^2}[\bar{u}(p_{11})\slashed{q}_4 P_L v(p_{10})][\bar{u}(p_9)\slashed{q}_4 P_L iS_F(p_3)] \right\}
$$

(6.16)

Next, we take the element B as

$$B = [\bar{u}(p_7) \times \frac{-i\alpha_w}{\sqrt{2}} \gamma^\kappa P_L \times v(p_8)] \times iD^W_{\beta\kappa}(q_3) \times [\bar{v}(p_6) \times \frac{-i\alpha_w}{\sqrt{2}} \gamma^\beta P_L \times iS_F(p_5)] \tag{6.17}$$

$$= [\bar{u}(p_7) \times \frac{-i\alpha_w}{\sqrt{2}} \gamma^\kappa P_L \times v(p_8)] \times iD^W_{\beta\kappa}(q_3) \times [u(p_6) \times \frac{-i\alpha_w}{\sqrt{2}} \gamma^\beta P_L \times iS_F(p_5)] \tag{6.18}$$

Note that this term has the same form of Equation 6.12, up to a minus sign. This obligates B to take the form

$$B = \frac{i\Pi(q_5)\alpha_w^2}{2} \left\{ [\bar{u}(p_7)\gamma_\beta P_L v(p_8)][u(p_6)\gamma^\beta P_L iS_F(p_5)] \cdots \right.$$
$$\left. \cdots - \frac{1}{m_w^2}[\bar{u}(p_7)\slashed{q}_3 P_L v(p_8)][u(p_6)\slashed{q}_3 P_L iS_F(p_5)] \right\} \tag{6.19}$$

Consequently, let us define the C factor as simply

$$E = iS_F(p_4) \times \frac{im_N}{2f}\gamma^5 \tag{6.20}$$

Before defining D, let us rewrite the pseudovector couplings of the Z boson, to a fermion f, as well as the coupling constant as

$$P_Z^f = (C_A^f - C_V^f \gamma^5); \quad \alpha_z = \frac{\alpha_w}{\sqrt{2}\cos\theta_W} \tag{6.21}$$

This lets us define the final element D as

$$D = iD^Z_{\mu\nu}(q_1) \times \frac{-i\alpha_z}{\sqrt{2}}\gamma^\nu(c_A^N - c_V^N\gamma^5) \times [\bar{v}(p_2) \times \frac{-i\alpha_z}{\sqrt{2}}\gamma^\mu(c_A^q - c_V^q\gamma^5) \times u(p_1)] \tag{6.22}$$

In terms of the projector, which was defined in Equation 6.21, as

$$D = -\frac{\alpha_z^2}{2} \times iD_{\mu\nu}(q_1)^Z \times \gamma^\nu P_z^N \times [\bar{v}(p_2)\gamma^\mu P_z^q u(p_1)] \tag{6.23}$$

For the Z boson propagator, let us define I(q)$= \frac{1}{q^2 - m_z^2}$. This implies that D takes the form

$$D = -\frac{i\alpha_Z^2 I(q_1)}{2} \left\{ \gamma^\mu P_z^N[\bar{v}(p_2)\gamma^\mu P_z^q u(p_1)] - \frac{1}{m_Z^2}\slashed{q}_1 P_z^N[\bar{v}(p_2)\slashed{q}_1 P_Z^q u(p_1)] \right\} \tag{6.24}$$

However, as the polarizations and spin values of the initial and final states are arbitrary, we are obligated to average over the initial states, and sum over the spins of the final ones. This means that we have to calculate the unpolarized matrix element as

$$\langle|\mathcal{M}|^2\rangle = \frac{1}{2}\sum_{spins} \mathcal{M}^*\mathcal{M} \tag{6.25}$$

To calculate the adjoint matrix element, we have first to calculate the adjoints of some of the currents. Let us begin with a pseudovector current

$$[\bar{u}\gamma^\mu P_L v]^\dagger = v^\dagger P_L^\dagger (\gamma^\mu)^\dagger \bar{u}^\dagger \tag{6.26}$$

$$= v^\dagger P_L \gamma^0 \gamma^\mu \gamma^0 \gamma^0 u \tag{6.27}$$

$$= \bar{v} P_R \gamma^\mu u \tag{6.28}$$

where $P_R = \frac{1}{2}(1 + \gamma^5)$. Now, for the other possible current we have

$$[u\gamma^\beta P_L i S_F]^\dagger = [\bar{v}\gamma^\beta P_L i S_F]^\dagger \tag{6.29}$$

$$= -iS_F^\dagger P_L \gamma^0 \gamma^\beta \gamma^0 \gamma^0 v \tag{6.30}$$

$$= -iS_F^\dagger \gamma^0 P_R \gamma^\beta \bar{u} \tag{6.31}$$

$$= -\gamma^0 i S_F P_R \gamma^\beta \bar{u} \tag{6.32}$$

Finally, for the Z current we have

$$[\bar{v}\gamma^\mu P_z^f u]^\dagger = u^\dagger (P_z^f)^\dagger (\gamma^\mu)^\dagger \bar{v}^\dagger \tag{6.33}$$

$$= u^\dagger P_z^f \gamma^0 \gamma^\mu \gamma^0 \gamma^0 v \tag{6.34}$$

$$= u^\dagger P_z^f \gamma^0 \gamma^\mu v \tag{6.35}$$

$$= u^\dagger (C_V^f - C_A^f \gamma^5) \gamma^0 \gamma^\mu v \tag{6.36}$$

$$= u^\dagger \gamma^0 (C_V^f + C_A^f \gamma^5) \gamma^\mu v \tag{6.37}$$

$$= \bar{u} P_{z,+}^f \gamma^\mu v \tag{6.38}$$

This being established, we have that the conjugated matrix element is given by

$$i\mathcal{M}^* = D^* \times E^* \times B^* \times A^* \tag{6.39}$$

With each term given by

$$D^* = -\frac{i\alpha_Z^2 I(q_1)}{2}\left\{ [\bar{u}(p_1) P_{z,+}^q \gamma^\mu v(p_2) P_z^N \gamma_\mu] - \frac{1}{m_Z^2}[\bar{u}(p_1) P_{z,+} \slashed{q}_1 v(p_2) P_z^N \slashed{q}_1] \right\} \tag{6.40}$$

For C we have:

$$E^* = \frac{im_N}{2f}\gamma^5 \gamma^0 i S_F(p_4) \gamma^0 \tag{6.41}$$

Now, for B:

$$B^* = \frac{i\Pi(q_5)\alpha_W^2}{2}\left\{ [iS_F(p_5) P_R \gamma^\beta \bar{u}(p_6)][\bar{v}(p_8) P_R \gamma_\beta u(p_7)] - \frac{1}{m_W^2}\cdots \right.$$
$$\left. \cdots [iS_F(p_5) P_R \slashed{q}_3 \bar{u}(p_6)][\bar{v}(p_8) P_R \slashed{q}_3 u(p_7)] \right\} \tag{6.42}$$

Finally, for A we have

$$A^* = \frac{-i\Pi(q_4)\alpha_W^2}{2}\left\{[iS_F(p_3)P_R\gamma^\eta u(p_9)][\bar{v}(p_{10})P_R\gamma_\eta u(p_{11})]\cdots\right.$$
$$\left.\cdots - \frac{1}{m_W^2}[iS_F(p_3)P_R\slashed{q}_3 u(p_9)][\bar{v}(p_{10})P_R\slashed{q}_4 u(p_{11})]\right\} \tag{6.43}$$

This means that the spin averaged matrix element takes the form

$$\langle|\mathcal{M}|^2\rangle = \frac{1}{2}\sum_{spins}(D^* \times E^* \times B^* \times A^*)(A \times B \times E \times D) \tag{6.44}$$

To make these calculations, first let us calculate the product $A^* \times A$. Before of it, let us define the parameter

$$a^2(q_4) = -\frac{\Pi^2(q_4)\alpha_W^4}{4} \tag{6.45}$$

Hence,

$$\sum_{spins}A^*A = a^2\sum_{spins}\left[iS_F(p_3)P_R\gamma^\eta u(p_9)][\bar{v}(p_{10})P_R\gamma_\eta u(p_{11})] - \cdots\right.$$
$$\cdots - \frac{1}{m_W^2}[iS_F(p_3)P_R\slashed{q}_4 u(p_9)][\bar{v}(p_{10}P_R\slashed{q}_4 u(p_{11})]\right\} \times \cdots$$
$$\cdots \times \left\{[\bar{u}(p_{11})\gamma_\lambda P_L v(p_{10})][\bar{u}(p_9)\gamma^\lambda P_L iS_F(p_3)] - \cdots\right.$$
$$\cdots - \frac{1}{m_W^2}[\bar{u}(p_{11})\slashed{q}_4 P_L v(p_{10})][\bar{u}(p_9)\slashed{q}_4 P_L iS_F(p_3)]\right\}$$

As each term has implicit sums over spin states, we can move terms such that

$$\sum_{spins}A^*A = a^2\sum_{spins}\left\{[iS_F(p_3)P_R\gamma^\eta u(p_9)\bar{u}(p_9)\gamma^\lambda P_L iS_F(p_3)] \times \cdots\right.$$
$$\cdots \times [\bar{v}(p_{10})P_R\gamma_\eta u(p_{11})\bar{u}(p_{11})\gamma_\lambda P_L v(p_{10})] - \cdots$$
$$\cdots - \frac{1}{m_W^2}[\bar{v}(p_{10})P_R\gamma_\eta u(p_{11})\bar{u}(p_{11})\slashed{q}_4 P_L v(p_{10})] \times \cdots$$
$$\cdots \times [iS_F(p_3)P_R\gamma^\eta u(p_9)\bar{u}(p_9)\slashed{q}_4 P_L iS_F(p_3)] - \cdots$$
$$\cdots - \frac{1}{m_W^2}[\bar{v}(p_{10})P_R\slashed{q}_4 u(p_{11})\bar{u}(p_{11})\gamma_\lambda P_L v(p_{10})] \times \cdots \tag{6.46}$$
$$\cdots \times [iS_F(p_3)P_R\slashed{q}_4 u(p_9)\bar{u}(p_9)\gamma_\lambda P_L iS_F(p_3)] + \cdots$$
$$\cdots + \frac{1}{m_W^4}[iS_F(p_3)P_R\slashed{q}_4 u(p_9)\bar{u}(p_9)\slashed{q}_4 P_L iS_F(p_3)] \times \cdots$$
$$\cdots \times [\bar{u}(p_{10})P_R\slashed{q}_4 u(p_{11})\bar{u}(p_{11})\slashed{q}_4 P_L v(p_{10})]\right\}$$

Our next step is to use the identities

$$\sum_r u_{r\alpha}(p)\bar{u}_{r\beta} = (\not{p} + m)_{\alpha\beta}; \quad \sum_r v_{r\alpha}\bar{v}_{r\beta} = (\not{p} - m)_{\alpha\beta} \tag{6.47}$$

After taking the sums, all terms will be nothing but traces, such that

$$
\begin{aligned}
\sum_{spins} A^*A =a^2\Big\{ &\operatorname{tr}[iS_F(p_3)P_R\gamma^\eta(\not{p}_9 + m_1)\gamma^\lambda P_L iS_F(p_3)] \times \cdots \\
&\cdots \times \operatorname{tr}[(\not{p}_{10} - m_2)P_r\gamma_\eta(\not{p}_{11} + m_{\nu1})P_L] - \cdots \\
&\cdots - \frac{1}{m_W^2} \operatorname{tr}[(\not{p}_{10} - m_2)P_R\gamma_\eta(\not{p}_{11} + m_{\nu1})\not{q}_4 P_L] \times \cdots \\
&\cdots \times \operatorname{tr}[iS_F(p_3)P_R\gamma^\eta(\not{p}_9 + m_1)\not{q}_4 P_L iS_F(p_3)] - \cdots \\
&\cdots - \frac{1}{m_W^2} \operatorname{tr}[(\not{p}_{10} - m_2)P_R\not{q}_4(\not{p}_{11} + m_{\nu1})\gamma_\lambda P_L] \times \cdots \\
&\cdots \times \operatorname{tr}[iS_F(p_3) \times P_R\not{q}_4(\not{p}_9 + m_1)\gamma_\lambda P_L iS_F(p_3)] - \cdots \\
&\cdots - \frac{1}{m_W^4} \operatorname{tr}[\gamma^0 iS_F(p_3)P_R\not{q}_4(\not{p}_9 + m_1)\not{q}_4 P_L iS_F(p_3)] \times \cdots \\
&\cdots \times \operatorname{tr}[(\not{p}_{10} - m_2)P_R\not{q}_4(\not{p}_{11} + m_{\nu1})\not{q}_4 P_L v(p_{10})]\Big\}
\end{aligned} \tag{6.48}
$$

Consequently, for the product of B^* and B, we have the same structure. This means, that we already know it's result by the means of Equation 6.48, but as we are changing the momenta, we first define

$$b^2 = -\frac{\Pi(q_5)^2\alpha_W^4}{4} \tag{6.49}$$

Such that we obtain the traces

$$
\begin{aligned}
\sum_{spins} B^*B =b^2\Big\{ &\operatorname{tr}[iS_F(p_5)P_R\gamma^\beta(\not{p}_6 - m_3)\gamma^\alpha P_L iS_F(p_5)] \times \cdots \\
&\cdots \times \operatorname{tr}[(\not{p}_8 - m_{\nu2})P_R\gamma_\beta(\not{p}_7 + m_4)\gamma_\alpha P_L] - \cdots \\
&\cdots - \frac{1}{m_W^2} \operatorname{tr}[iS_F(p_5)P_R\gamma^\beta(\not{p}_6 - m_3)\not{q}_3 P_L iS_F(p_5)] \times \cdots \\
&\cdots \times \operatorname{tr}[(\not{p}_8 - m_{\nu2})P_R\gamma_\beta(\not{p}_7 + m_4)\not{q}_3 P_L] - \cdots \\
&\cdots - \frac{1}{m_W^2} \operatorname{tr}[iS_F(p_5)P_R\not{q}_3(\not{p}_6 - m_3)\gamma^\alpha P_L iS_F(p_5)] \times \cdots \\
&\cdots \times \operatorname{tr}[(\not{p}_8 - m_{\nu2})P_R\not{q}_3(\not{p}_7 + m_4)\gamma_\alpha P_L] + \cdots \\
&\cdots + \frac{1}{m_W^4} \operatorname{tr}[iS_F(p_5)P_R\not{q}_3(\not{p}_6 - m_3)\not{q}_3 P_L iS_F(p_5)] \times \cdots \\
&\cdots \times \operatorname{tr}[(\not{p}_8 - m_{\nu2})P_R\not{q}_3(\not{p}_7 + m_4)\not{q}_3 P_L]\Big\}
\end{aligned} \tag{6.50}
$$

For the E^*E product we first define

$$c^2 = -\frac{m_N^2}{4f^2} \tag{6.51}$$

$$\sum_{spins} E^*E = c^2 \operatorname{tr}[\gamma^0 i S_F(p_4)\gamma^0 i S_F(p_4)] \tag{6.52}$$

Finally, for the D^*D we define

$$d^2 = -\frac{\alpha_Z^4 I(q_1)^2}{4} \tag{6.53}$$

such that the traces become

$$
\begin{aligned}
\sum_{spins} D^*D = d^2 \Big\{ &\operatorname{tr}[(\not{p}_1 + m_{q1})P_{Z+}^q \gamma^\mu (\not{p}_2 - m_{q2})P_Z^N \gamma_\mu \gamma_\nu P_Z^N \gamma^\nu P_Z^q] - \cdots \\
\cdots &- \frac{1}{m_W^2}\operatorname{tr}[(\not{p}_1 + m_{q1})P_{Z+}^q \gamma^\mu (\not{p}_2 - m_{q2})P_Z^N \gamma_\mu \not{q}_1 P_Z^N \not{q}_1 P_Z^q] - \cdots \\
\cdots &- \frac{1}{m_W^2}\operatorname{tr}[(\not{p}_1 + m_{q1})P_{Z+}^q \not{q}_1 (\not{p}_2 - m_{q2})P_Z^N \not{q}_1 \gamma_\nu P_Z^N \gamma^\nu P_Z^q] + \cdots \\
\cdots &+ \frac{1}{m_W^4}\operatorname{tr}[(\not{p}_1 + m_{q1})P_{Z+}^q \not{q}_1 (\not{p}_2 - m_{q2})P_Z^N \not{q}_1 \not{q}_1 P_Z^N \not{q}_1 P_Z^q] \Big\}
\end{aligned} \tag{6.54}
$$

7. Calculation of the production matrix element of a Majoron via VBF.

After momentum assignation in all vertices, the Feynman diagram is that of Figure 7.1.
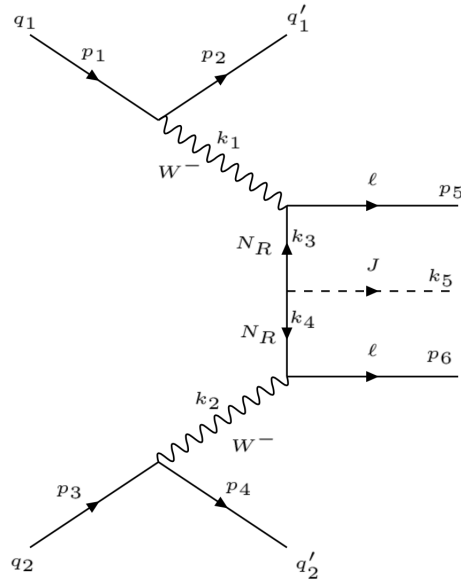
Figure 7.1: Feynman diagram of VBF production of a J after momentum assignation.

Following the same steps of our previous calculation, we set momentum conservation rules

$$p_1 = p_2 + k_1 \tag{7.1}$$
$$k_1 = k_3 + p_5 \tag{7.2}$$
$$k_5 = k_3 - k_4 \tag{7.3}$$
$$k_2 = p_3 - p_4 \tag{7.4}$$
$$k_2 = p_4 + p_6 \tag{7.5}$$

After a little algebra we get

$$k_5 = p_1 + p_4 + p_6 - p_2 - p_3 - p_4 \tag{7.6}$$

After establishing our momentum conservation equation, we proceed to write the matrix element

as

$$-i\mathcal{M} = [\bar{u}(p_2) \times \frac{-i\alpha_w}{\sqrt{2}} \gamma^\mu P_L \times u(p_1)] \times iD_{\mu\nu}^W(k_1) \times \cdots$$
$$\cdots \times [v(p_5) \times \frac{-i\alpha_w}{\sqrt{2}} \gamma^\nu P_L \times iS_F(k_3)] \times \frac{im_N}{2f} \gamma_5 \times \cdots$$
$$\cdots \times [v(p_6) \times \frac{-i\alpha_w}{\sqrt{2}} \gamma^\alpha P_L \times iS_F(k_4)] \times iD_{\alpha\beta}^W(k_2) \times \cdots \tag{7.7}$$
$$\cdots \times [\bar{u}(p_4) \times \frac{-i\alpha_w}{\sqrt{2}} \alpha^\beta P_L \times u(p_3)]$$

Let us consider that the matrix element in Equation 7.7 can be written as a product of three terms,

$$-i\mathcal{M} = A \times B \times C. \tag{7.8}$$

where each of them is given by:

$$A = [\bar{u}(p_2) \times \frac{-i\alpha_w}{\sqrt{2}} \gamma^\mu P_L \times u(p_1)] \times iD_{\mu\nu}^W(k_1) \times [v(p_5) \times \frac{-i\alpha_w}{\sqrt{2}} \gamma^\nu P_L \times iS_F(k_3)]$$
$$B = \frac{im_N}{2f} \gamma_5 \tag{7.9}$$
$$C = [v(p_6) \times \frac{-i\alpha_w}{\sqrt{2}} \gamma^\alpha P_L \times iS_F(k_4)] \times iD_{\alpha\beta}^W(k_2) \times [\bar{u}(p_4) \times \frac{-i\alpha_w}{\sqrt{2}} \alpha^\beta P_L \times u(p_3)]$$

After expanding the W boson progator we obtain:

$$A = \frac{-i\Pi(k_1)\alpha_w^2}{2} \left\{ [\bar{u}(p_2)\gamma^\mu P_L u(p_1)][v(p_5)\gamma_\mu P_L iS_F(k_3)] - \cdots \right.$$
$$\left. \cdots - \frac{1}{m_W^2} [\bar{u}(p_2)\not{k}_1 P_L u(p_1)][v(p_5)\not{k}_1 P_L iS_F(k_3)] \right\} \tag{7.10}$$

$$B = \frac{im_N}{2f}\gamma_5 \tag{7.11}$$

$$C = \frac{-i\Pi(k_2)\alpha_w^2}{2} \left\{ [v(p_6)\gamma^\alpha P_L iS_F(k_4)][\bar{u}(p_4)\gamma_\alpha P_L u(p_3)] - \cdots \right.$$
$$\frac{1}{m_W^2} [v(p_6)\not{k}_2 P_L iS_F(k_4)][\bar{u}(p_4)\not{k}_2 P_L u(p_3)] \tag{7.12}$$

As we're dealing with Majorana neutrinos, we can take them as Dirac ones, but flipping the u's and the v's of their corresponding leptons. Now, to calculate the conjugated matrix element, we

need the following identities

$$\begin{aligned}
[\bar{u}\gamma^\mu P_L u]^\dagger &= u^\dagger P_L \gamma^{\mu\dagger}\bar{u}^\dagger \\
&= u^\dagger P_L \gamma^0 \gamma^\mu \gamma^0 \gamma^0 u \\
&= u^\dagger P_L \gamma^0 \gamma^\mu u \\
&= \bar{u} P_R \gamma^\mu u
\end{aligned} \tag{7.13}$$

$$\begin{aligned}
[v\gamma_\mu P_L iS_F]^\dagger &= [\bar{u}\gamma_\mu P_L iS_F]^\dagger \\
&= -iS_F^\dagger P_L^\dagger \gamma_\mu^\dagger \bar{u}^\dagger \\
&= -i\gamma^0 S_F \gamma^0 P_L \gamma^0 \gamma_\mu \gamma^0 \gamma^0 u \\
&= -i\gamma^0 S_F P_R \gamma_\mu u \\
&= -\gamma^0 iS_F P_R \gamma_\mu \bar{v}
\end{aligned} \tag{7.14}$$

With this two identities we can calculate all conjugates of A, B and C. For A we have

$$A^* = \frac{i\Pi(k_1)\alpha_w^2}{2}\left\{[v(p_5)\gamma_\mu P_L iS_F(k_3)]^\dagger [\bar{u}(p_2)\gamma^\mu P_L u(p_1)]^\dagger \right. \tag{7.15}$$

After using the identities we have

$$\begin{aligned}
A^* =& \frac{-i\Pi(k_1)\alpha_w^2}{2}\left\{[iS_F(k_3)P_R\gamma_\mu\bar{v}(p_5)][\bar{u}(p_1)P_R\gamma^\mu u(p_2)] - \cdots \right. \\
& \left. -\frac{1}{m_W^2}[iS_F(k_3)P_R\slashed{k}_1\bar{v}(p_5)][\bar{u}(p_1)P_R\slashed{k}_1 u(p_2)]\right\}
\end{aligned} \tag{7.16}$$

For B we obtain a simple expression

$$B^* = -\frac{im_N}{2f}\gamma_5 \tag{7.17}$$

Finally, for C we obtain

$$\begin{aligned}
C^* =& -\frac{i\Pi(k_2)\alpha_w^2}{2}\left\{[\bar{u}(p_3)P_R\gamma_\alpha u(p_4)][iS_F(k_4)P_R\gamma^\alpha\bar{v}(p_6)] - \cdots \right. \\
& \left. -\frac{1}{m_W^2}[\bar{u}(p_3)P_R\slashed{k}_2 u(p_4)][iS_F(k_4)P_R\slashed{k}_2\bar{v}(p_6)]\right\}
\end{aligned} \tag{7.18}$$

Before calculating the spin averaged matrix element, let us define the momentum variables

$$a^2 = -\frac{\Pi(k_1)^2 \alpha_w^4}{4} \qquad\qquad b^2 = -\frac{m_N^2}{4f^2} \qquad\qquad c^2 = -\frac{\Pi(k_2)^2 \alpha_w^4}{4} \qquad (7.19)$$

Our spin averaged matrix element will be given by

$$\langle |\mathcal{M}|^2 \rangle = \frac{1}{2} \sum_{spins} (C^* \times B^* \times A^*)(A \times B \times C) \qquad (7.20)$$

Our first product is the one relating the A's. This product is given by

$$
\begin{aligned}
\sum_{spins} A^* A =& a^2 \sum_{spins} \left\{ [iS_F(k_3) P_R \gamma_\mu \bar{v}(p_5)][\bar{u}(p_1) P_R \gamma^\mu u(p_2)] - \cdots \right. \\
& \left. \frac{1}{m_W^2} [iS_F(k_3) P_R \slashed{k}_1 \bar{v}(p_5)][\bar{u}(p_1) P_R \slashed{k}_1 u(p_2)] \right\} \times \\
& \left\{ [\bar{u}(p_2) \gamma^\nu P_L u(p_1)][v(p_5) \gamma_\nu P_L iS_F(k_3)] - \cdots \right. \\
& \left. \frac{1}{m_W^2} [\bar{u}(p_2) \slashed{k}_1 P_L u(p_1)][v(p_5) \slashed{k}_1 P_L iS_F(k_3)] \right\}
\end{aligned}
\qquad (7.21)
$$

Note that in the products we will obtain products of the form $\bar{v} \times v$. To deal with them we use the Majorana property mentioned in our previous calculation; this turns the product to $u \times \bar{u}$:

$$
\begin{aligned}
\sum_{spins} A^* \times A =& a^2 \gamma^0 \left\{ [iS_F(k_3) P_R \gamma_\mu u(p_5) \bar{u}(p_5) \gamma_\nu P_L iS_F(k_3)] \times \cdots \right. \\
& \cdots [\bar{u}(p_1) P_R \gamma^\mu u(p_2) \bar{u}(p_2) \gamma^\nu P_L u(p_1)] - \cdots \\
& \cdots - \frac{1}{m_W^2} [iS_F(k_3) P_R \gamma_\mu u(p_5) \bar{u}(p_5) \slashed{k}_1 P_L iS_F(k_3)] \times \cdots \\
& \cdots [\bar{u}(p_1) P_R \gamma^\mu u(p_2) \bar{u}(p_2) \slashed{k}_1 P_L u(p_1)] - \cdots \\
& - \cdots \frac{1}{m_W^2} [iS_F(k_3) P_R \slashed{k}_1 u(p_5) \bar{u}(p_5) \gamma_\nu P_L iS_F(k_3)] \times \cdots \\
& \cdots [\bar{u}(p_1) P_R \slashed{k}_1 u(p_2) \bar{u}(p_2) \gamma^\nu P_L u(p_1)] + \cdots \\
& \cdots + \frac{1}{m_W^4} [iS_F(k_3) P_R \slashed{k}_1 u(p_5) \bar{u}(p_5) \slashed{k}_1 P_L iS_F(k_3)] \times \cdots \\
& \left. \cdots [\bar{u}(p_1) P_R \slashed{k}_1 u(p_2) \bar{u}(p_2) \slashed{k}_1 P_L u(p_1)] \right\}
\end{aligned}
\qquad (7.22)
$$

So, after performing the sum, and using Equation 6.47 we obtain

$$
\begin{aligned}
\sum_{spins} A^*A = a^2 \Big\{ & \text{tr}[iS_F(k_3)P_R\gamma_\mu(\slashed{p}_5 + m_3)\gamma_\nu P_L iS_F(k_3)] \times \cdots \\
& \cdots \text{tr}[(\slashed{p}_1 + m_1)P_R\gamma^\mu(\slashed{p}_2 + m_2)\gamma_\nu P_L] - \cdots \\
& \cdots - \frac{1}{m_W^2}\text{tr}[iS_F(k_3)P_R\slashed{k}_1(\slashed{p}_5 + m_3)\gamma_\nu P_L iS_F(k_3)] \times \cdots \\
& \cdots \text{tr}[(\slashed{p}_1 + m_1)P_R\slashed{k}_1(\slashed{p}_2 + m_2)\gamma^\nu P_L] - \cdots \\
& \cdots - \frac{1}{m_W^2}\text{tr}[iS_F(k_3)P_R\gamma_\mu(\slashed{p}_5 + m_3)\slashed{k}_1 P_L iS_F(k_3)] \times \cdots \\
& \cdots \times \text{tr}[(\slashed{p}_1 + m_1)P_R\gamma^\mu(\slashed{p}_2 + m_2)\slashed{k}_1 P_L] + \cdots \\
& \cdots + \frac{1}{m_W^4}\text{tr}[iS_F(k_3)P_R\slashed{k}_1(\slashed{p}_5 + m_3)\slashed{k}_1 P_L iS_F(k_3)] \times \cdots \\
& \cdots \times \text{tr}[(\slashed{p}_1 + m_1)P_R\slashed{k}_1(\slashed{p}_2 + m_2)\slashed{k}_1 P_L] \Big\}
\end{aligned}
\tag{7.23}
$$

Secondly, for the product of B and it's conjugated:

$$
\begin{aligned}
\sum_{spins} B^*B &= b^2 \sum_{spins} (\gamma_5)^2 \\
&= b^2 \sum_{spins} \mathbb{1} \\
&= 4b^2
\end{aligned}
\tag{7.24}
$$

Finally, as C follows the same structure of A, we can extrapolate it's results such that we get

$$
\begin{aligned}
\sum_{spins} C^*C = c^2 \Big\{ & \text{tr}[(\slashed{p}_3 + m_5)P_R\gamma_\alpha(\slashed{p}_4 + m_6)\gamma_\beta P_L] \times \cdots \\
& \cdots \times \text{tr}[iS_F(k_4)P_R\gamma^\alpha(\slashed{p}_6 + m_4)\gamma^\beta P_L iS_F(k_4)] - \cdots \\
& \cdots - \frac{1}{m_W^2}\text{tr}[(\slashed{p}_3 + m_5)P_R\gamma_\alpha(\slashed{p}_4 + m_6)\slashed{k}_2 P_L] \times \cdots \\
& \cdots \times \text{tr}[iS_F(k_4)P_R\gamma^\alpha(\slashed{p}_6 + m_4)\slashed{k}_2 P_L iS_F(k_4)] - \cdots \\
& \cdots - \frac{1}{m_W^2}\text{tr}[(\slashed{p}_3 + m_5)P_R\slashed{k}_2(\slashed{p}_4 + m_6)\gamma_\beta P_L] \times \cdots \\
& \cdots \times \text{tr}[iS_F(k_4)P_R\slashed{k}_2(\slashed{p}_6 + m_4)\gamma^\beta P_L iS_F(k_4)] + \cdots \\
& \cdots + \frac{1}{m_W^4}\text{tr}[(\slashed{p}_3 + m_5)P_R\slashed{k}_2(\slashed{p}_4 + m_6)\slashed{k}_2 P_L] \times \cdots \\
& \cdots \times \text{tr}[iS_F(k_4)P_R\slashed{k}_2(\slashed{p}_6 + m_4)\slashed{k}_2 P_L iS_F(k_4)] \Big\}
\end{aligned}
\tag{7.25}
$$

8. Calculation of the production matrix element of a Majoron via W channel

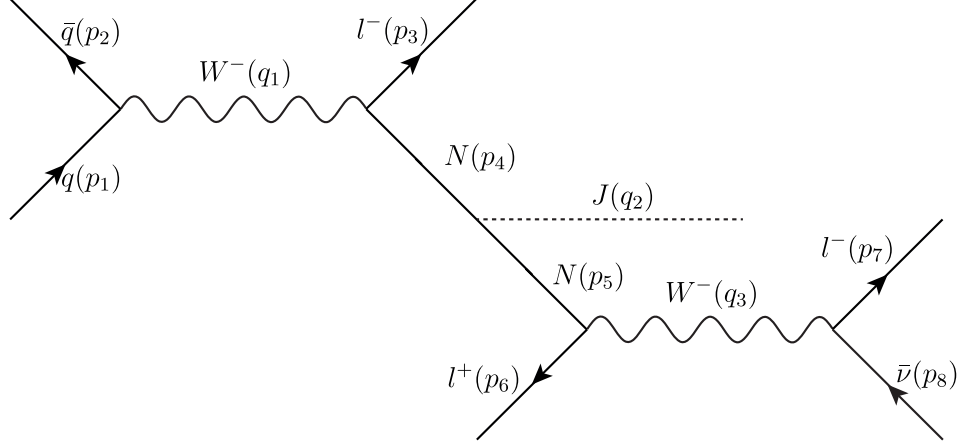After momentum assignation in every vertex, the Feynman diagram is that of Figure 8.1.

Figure 8.1: Feynman diagram of W-channel production of a J after momentum assignation.

Following the same steps of our previous two calculations, we obtain the following momentum conservation rules

$$p_1 - p_2 = q_1 \tag{8.1}$$

$$q_1 = p_3 + p_4 \tag{8.2}$$

$$q_2 = p_4 - p_5 \tag{8.3}$$

$$p_5 - p_6 = q_3 \tag{8.4}$$

$$q_3 = p_7 + p_8 \tag{8.5}$$

After a little algebra we obtain that this radiating process must obey

$$q_2 = p_1 - p_2 - p_3 - p_6 - p_7 - p_8. \tag{8.6}$$

By using the same Feynman rules as before, we get that the Feynman amplitude is given by

$$
\begin{aligned}
i\mathcal{M} =& \frac{im_N g_w^4}{8f} [\bar{u}(p_7)\gamma^\mu P_L v(p_8)] i D_{\mu\nu}(q_3) [u(p_6)\gamma^\nu P_L i S_F(p_5)]\gamma_5 [v(p_3)\gamma^\alpha P_L i S_F(p_4)] \times \cdots \\
& \cdots \times i D_{\alpha\beta}(q_1)[\bar{v}(p_2)\gamma^\beta P_L u(p_1)]
\end{aligned}
\tag{8.7}
$$

If we take the W boson to be off-shell such that $m_w >> p$ we can reduce the propagator to

$$iD_{\mu\nu(q)} = -i\frac{\eta_{\mu\nu} - \frac{q_\mu q_\nu}{m_w^2}}{p^2 - m_w^2} \rightarrow i\frac{\eta_{\mu\nu}}{m_w^2} \tag{8.8}$$

Hence

$$i\mathcal{M} = \frac{-im_N g_w^4}{8fm_w^4}[\bar{u}(p_7)\gamma^\mu P_L v(p_8)][u(p_6)\gamma_\mu P_L iS_F(p_5)]\gamma_5[v(p_3)\gamma^\alpha P_L iS_F(p_4)][\bar{v}(p_2)\gamma_\alpha P_L u(p_1)] \tag{8.9}$$

The adjoint matrix is then

$$-i\mathcal{M}^\dagger = \frac{-im_N g_w^4}{8fm_w^4}[\bar{u}(p_1)P_R\gamma^\delta v(p_2)][iS_F(p_4)P_R\gamma_\delta\bar{v}(p_3)]\gamma_5[iS_F(p_5)P_R\gamma_\rho\bar{u}(p_6)][\bar{v}(p_8)P_R\gamma^\rho u(p_7)]$$

$$\tag{8.10}$$

9. Phenomenological Analysis

A feasibility study for the production of HN and J bosons at the LHC was performed, considering purely diagonal couplings between leptons and neutrinos. The model was implemented in the software Mathematica, using the FeynRules package [75]. The package produces the so called Universal FeynRules Output (UFO), which is used as input for the software MadGraph [76]. This software allows the emulation of proton-proton collisions at the center of momentum energy at the LHC. In addition, it allows to simulate the desired final states for both, SM processes, also known as backgrounds, and signal processes of interest. Background and signal events were generated using a 13 TeV proton-proton collision energy. The associated fragmentation processes of partons (quarks and gluons) was produced using Pythia [77]. The fragmentation of partons is a consequence of the strong interaction. Pythia emulates the corresponding production of hadrons resulting from this process. This is also referred to as hadronization. The simulation of the interaction between particles and a generic particle-physics detector at the LHC, was included using the software Delphes [78]. This software includes associated efficiencies, misidentification rates, momentum and energy resolution effects, which are known experimental effects. The input card associated to the characteristics of the CMS detector was used in all the simulations.

Background processes with similar final states as those considered for the expected signals were considered. Production of Drell-Yan events, Z/γ^*, with associated jets from initial state ration, and of W-bosons with associated jets, referred to as V+jets were included. Additionally, events with two (WW. WZ, ZZ) or three vector bosons (WWW, WWZ, WZZ, ZZZ) were also included. These events are represented as VV and VVV, respectively. Finally, production of top-anti-top pairs were also simulated. Table 9.1 shows the number of events simulated for the backgrounds.

Table 9.1: Number of events produced for the backgrounds.

Background	N_e
$t\bar{t}$	24.307.250
W+jets	20.925.778
Z+jets	18.505.572
WWW	5.000.000
WWZ	2.500.000
ZZW	2.500.000
ZZZ	5.000.000
WW	12.500.000
WZ	9.850.000
ZZ	10.000.000

9.1 W channel production

The first set of signal samples produced were generated for the W-channel. Scenarios where the mass difference between the Majoron and the lightest neutrino (N_e) is 100 GeV ($\Delta m(N_e, J) = 100$ GeV) and where the following mass differences hold: $\Delta m(N_e, J) = \Delta m(N_e, N_\mu) = \Delta m(N_\mu, N_\tau)$, were considered. The complete mass spectra explored in the analysis, is presented in Table 9.2. The signal samples simulation considered the processes: $\text{p p} \to \bar{\nu}_\tau\ \tau^+\ \text{J}\ \tau^-\ \tau^+$, $\text{p p} \to \bar{\nu}_\mu\ \mu^+\ \text{J}\ \mu^-\ \mu^+$ and $\text{p p} \to \bar{\nu}_e\ e^+\ \text{J}\ e^-\ e^+$.

The syntax used to produced the signal samples in MadGraph is presented next:

```
> import model SM_HeavyN_UFO
> define lepton = e- mu- ta-
> define lepton~ = e+ mu+ ta+
> define neutrino = ve vm vt
> define neutrino~ = ve ~ vm ~ vt ~
> define p = u d u~ d~
> generate p p > lepton lepton~ j0 lepton neutrino~  QCD=0 QED<=5
```

Table 9.2: Number of events produced for the analyzed mass spectra.

{m(J), m(N_e), m(N_μ), and m(N_τ)}	Number of events
{50, 150, 250, 350}	200.000
{200, 300, 400, 500}	200.000
{700, 800, 900, 1000}	200.000

Figure 9.1 shows the production cross section as function of the tau-heavy-neutrino mass ($m(N_\tau)$). The blue curve shows the cross-section before decay, while the yellow curve shows the cross-section after decaying the N_τ. The difference between the curves is explained by the associated $W \to \tau\nu_\tau$ branching fraction. The cross-sections were obtained using MadGraph, and consistent values reported in other associated phenomenological studies for heavy neutrinos [79].
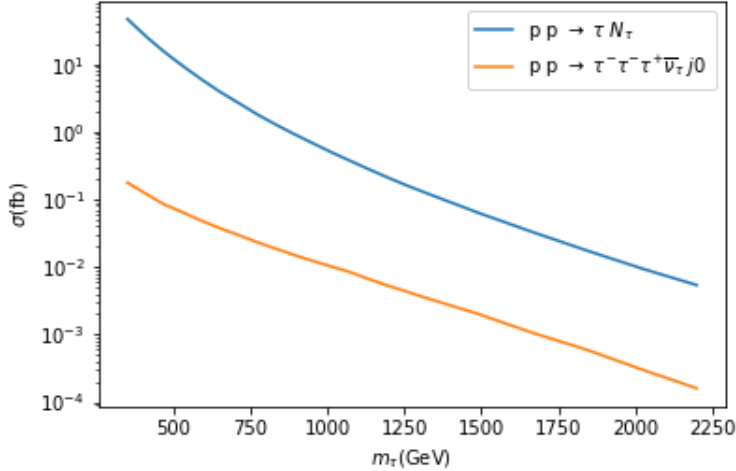
Figure 9.1: (Blue) Cross section as function of m(N_τ) considering production of stable neutrinos. (Yellow) Cross section considering Majoron radiation and non stable neutrinos.

9.1.1 Event Selection Criteria

To understand the kinematic and topological differences between the associated backgrounds and the signal, distributions normalized to unity are presented. The distributions were obtained after applying basic kinematic requirements on the transverse momentum (p_T) and pseudorapidiy (η), obtained from experimental studies reported at CMS and ATLAS [80, 81, 82].

Figure 9.2 show the p_T distribution for the electrons and muons. Note that signal events have signatures with higher p_T spectrum with respect to associated backgrounds. Figure 9.3 shows the missing transverse momentum distribution (p_T^{miss}). As expected, signal have higher values of p_T^{miss} with respect to backgrounds, because of the radiated Majoron and the associated neutrino from the leptonic decay of the W-boson. The transverse mass distribution between the highest p_T electron (muon) and the p_T^{miss} is shown on the left (right) in Figure 9.4. The transverse mass is defined as

$$m_T = \sqrt{2p_T(\ell)p_T^{miss} \times (1 - cos(\Delta\phi(\ell, p_T^{miss})))}$$

This variable is a well regarded experimental observable, widely used to observe the reconstructed mass of W-bosons (Jacobian peak). Note that the V+jets and $t\bar{t}$ backgrounds peak at around 80 GeV, which corresponds to the expected W-boson mass. For signal, the average large lepton-p_T and p_T^{miss}, naturally result in large m_T values. Figure 9.5 shows the difference in the azimuthal angle distribution, $\Delta\Phi$, between the highest p_T electron (muon) and the p_T^{miss}. Note that, as expected, the V+jets background (specially W+jets) and the signal peak at around π, which is expected given the nature of the topology of the decay. Finally, since signal events are characterized by object with large p_T and large p_T^{miss} values, we explored the so called S_T distribution, defined as the scalar sum of the p_T of all leptons and the p_T^{miss}. Figure 9.6 shows the S_T distribution. Note that this distribution gives a good signal-to-background separation.

58

Table 9.3: Basic Event Selection Criteria (I)

Criteria	Selections
$p_T(e)$	> 8 GeV
$p_T(\mu)$	> 5 GeV
$p_T(\tau)$	> 20 GeV
$|\eta(e)|, |\eta(\mu)|, |\eta(\tau)|$	< 2.4

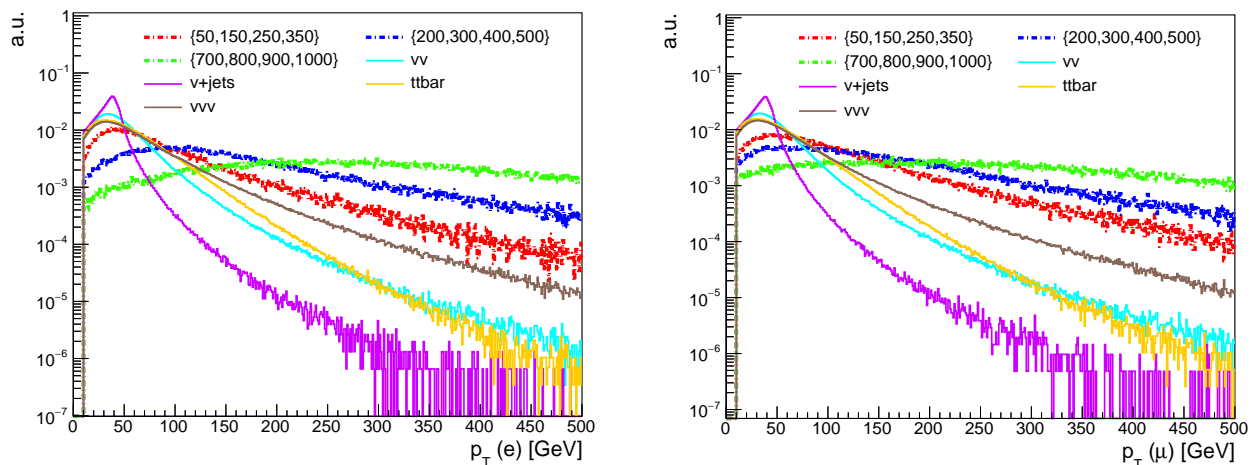Figure 9.2: Electrons (left) and muons (right) transverse momentum distribution in logarithmic scale. The notation for the signal samples correspond to $\{m(J), m(N_e), m(N_\mu), m(N_\tau)\}$.
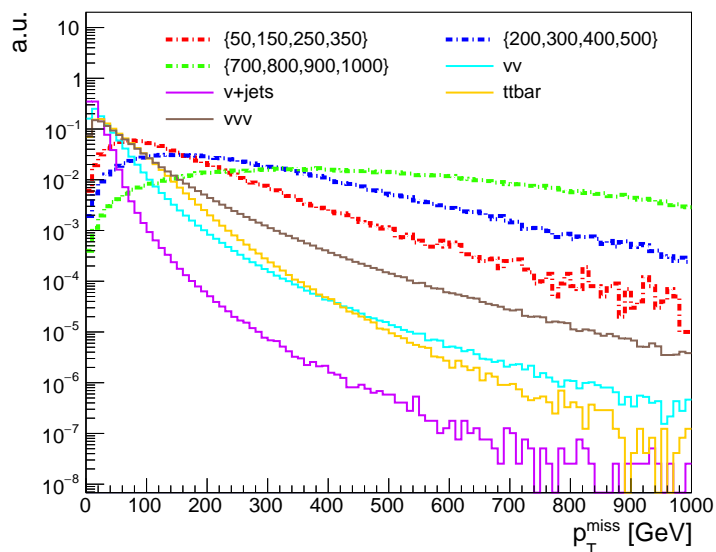
Figure 9.3: Missing energy transverse (E_T^{miss}) distribution for signal and backgrounds in logarithmic scale. The notation for the signal samples correspond to $\{m(J), m(N_e), m(N_\mu), m(N_\tau)\}$.

Figure 9.4: Electrons (left) and muons (right) transverse mass distribution in logarithmic scale. The notation for the signal samples correspond to $\{m(J), m(N_e), m(N_\mu), m(N_\tau)\}$.

Figure 9.5: Electrons (left) and muons (right) angular difference distribution. The notation for the signal samples correspond to $\{m(J), m(N_e), m(N_\mu), m(N_\tau)\}$.

Figure 9.6: ST distribution in logarithmic scale. The notation for the signal samples correspond to $\{m(J), m(N_e), m(N_\mu), m(N_\tau)\}$.
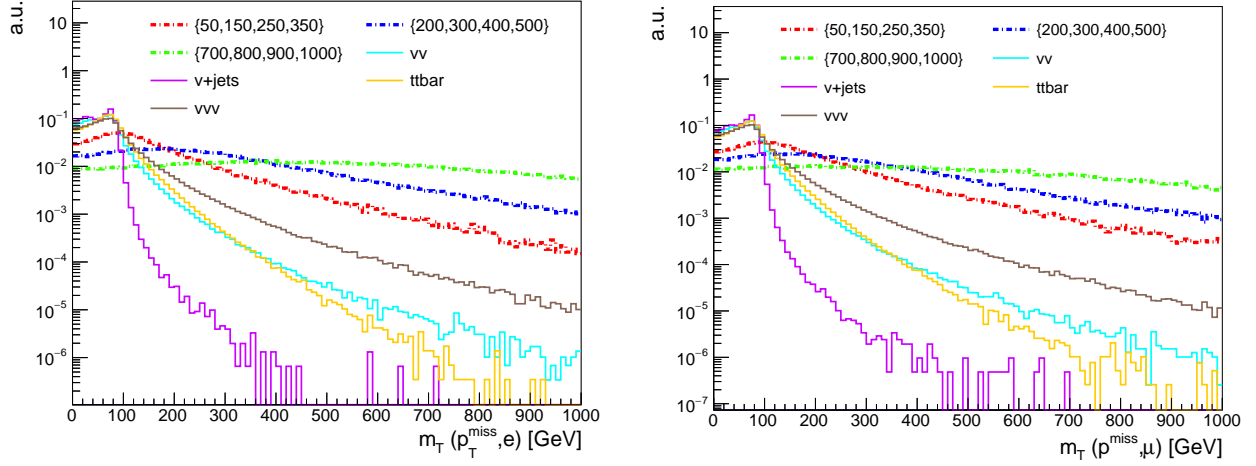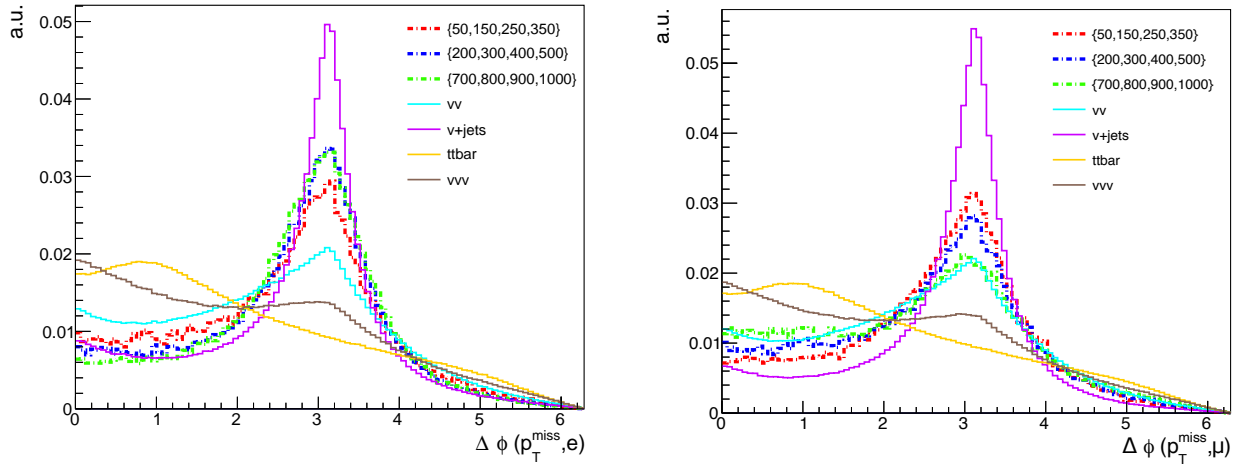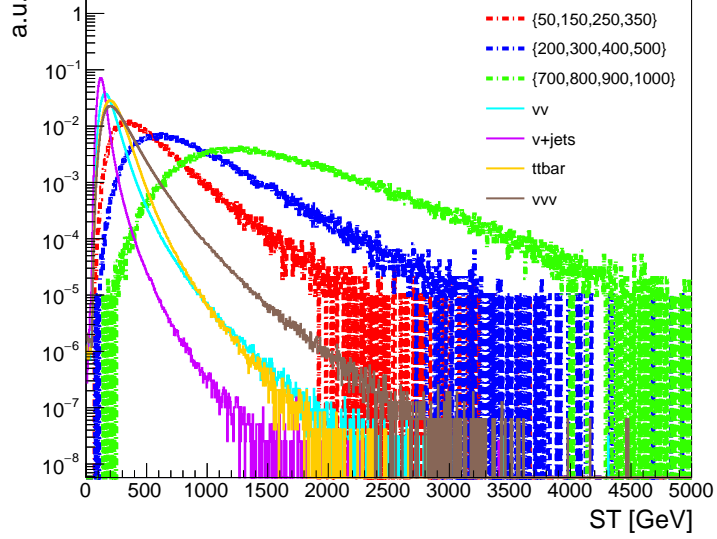
Table 9.4: Central Event Selection Criteria (II)

Criteria	Selections
p_T^{miss}	> 100 GeV
$N(b - jets)$	0
$p_T(\ell^{lead})$	> 50 GeV
$p_T(\ell^{other})$	> 20 GeV
$\Delta p_T(\ell^{lead}, \ell^{lowest})$	> 50 GeV

After analyzing various distributions a set of selection criteria was chosen to reduce the background contamination while keeping most of the signal events. Table 9.4 shows the chosen selection criteria. The requirement on p_T^{miss} and $\Delta p_T(\ell^{lead}, \ell^{lowest})$ respond to the features of the signal topology, the requirement on zero jets associated to b-quarks helps suppress the contribution from $t\bar{t}$ processes, and the minimum lepton p_T threshold is associated with experimental constrains related with thresholds for single-lepton triggers. The $\Delta p_T(\ell^{lead}, \ell^{lowest})$ requirement is defined as the absolute difference between in p_T between the lepton with the highest momentum (leading) and one with the lowest. After applying these selections, we considered four different final states, also referred to as channels: $\{e, e, \mu\}$ (CH1), $\{\mu, \mu, e\}$ (CH2), $\{\mu, \mu, \mu\}$ (CH3), and $\{e, e, e\}$ (CH4). The cumulative efficiencies of the different set of selections and channels are presented in Table 9.5. Efficiency ϵ_I corresponds to events passing the selections reported on Table 9.3, ϵ_{II} correspond to efficiencies after passing selections on Table 9.3 and Table 9.4, while ϵ_{III-VI} are associated to events passing selections on Table 9.3 and Table 9.4 for channels CH1-CH4.

after cuts I and II: (III) $\{e, e, \mu\}$, (IV) $\{\mu, \mu, e\}$, (V) $\{\mu, \mu, \mu\}$, (VI) $\{e, e, e\}$

61

Table 9.5: Percentage cumulative efficiencies for the signals and backgrounds after every cut.

Signals						
{m(J), m(N$_1$), m(N$_2$), m(N$_3$)}	ϵ_I	ϵ_{II}	ϵ_{III}	ϵ_{IV}	ϵ_V	ϵ_{VI}
{50, 150, 250, 350}	85.18	72.93	4.14	5.72	9.28	4.46
{200, 300, 400, 500}	95.52	86.51	8.22	5.69	6.89	8.59
{700, 800, 900, 1000}	99.01	92.53	12.13	4.86	4.89	11.26
Backgrounds						
Sample	ϵ_I	ϵ_{II}	ϵ_{III}	ϵ_{IV}	ϵ_V	ϵ_{VI}
www	41.56	29.44	4.47×10^{-2}	5.63×10^{-2}	3.84×10^{-2}	1.83×10^{-2}
zzw	43.36	28.94	6.81×10^{-2}	8.44×10^{-2}	15.29×10^{-2}	6.97×10^{-2}
zzz	41.41	26.62	4.15×10^{-2}	5.22×10^{-2}	7.13×10^{-2}	3.40×10^{-2}
wwz	47.51	32.52	8.76×10^{-2}	10.88×10^{-2}	15.58×10^{-2}	7.90×10^{-2}
wz	21.18	16.41	1.07×10^{-2}	1.44×10^{-2}	4.10×10^{-2}	2.85×10^{-2}
zz	20.00	15.66	2.13×10^{-3}	1.67×10^{-4}	8.26×10^{-3}	2.24×10^{-3}
ww	20.81	15.32	1.40×10^{-4}	4.00×10^{-5}	9.60×10^{-5}	2.32×10^{-4}
$t\bar{t}$	39.04	6.61	1.10×10^{-4}	1.73×10^{-4}	2.34×10^{-4}	1.60×10^{-4}
z+jets	2.79	2.54	5.40×10^{-6}	5.40×10^{-6}	-	5.4×10^{-6}
w+jets	3.89	2.99	-	-	-	-

Figure 9.7 shows the ST distribution for the eee channel (left) and for the $\mu\mu\mu$ channel (right), normalized to the production cross section and an expected luminosity of $1000 fb^{-1}$. The most relevant backgrounds are shown stacked while the signals are overlaid on top of the backgrounds. Note that the overall expected background is larger for the eee channel. Experimentally, electrons have lower identification efficiencies and higher miss-identification rates, with respect to muons. The miss identification rate can be up to one order of magnitude higher for electrons, depending on p_T. Although the background composition on the tail, where signal sensitivity is higher, seem different for both channel, note there are a few events falling in the high ST range, which have associated large statistical uncertainties. Nevertheless, it is important t o note that the event selection criteria chosen for this study, shows good potential to discriminate signal from background, showing that this analysis is feasible to be conducted at the LHC. A potential discovery might require larger luminosity to reach the 5σ statistical significance of a hypothetical observed signal, on top of the observed background. Therefore, this type of analysis might require the $3000 fb^{-1}$ of luminosity, expected to be collected by the end of the LHC physics program. Although the signal cross sections reported on this study are small, the unique topology of this search, which result in small backgrounds, and the expected luminosity during the LHC era, makes this analysis relevant to be conducted at ATLAS and CMS.
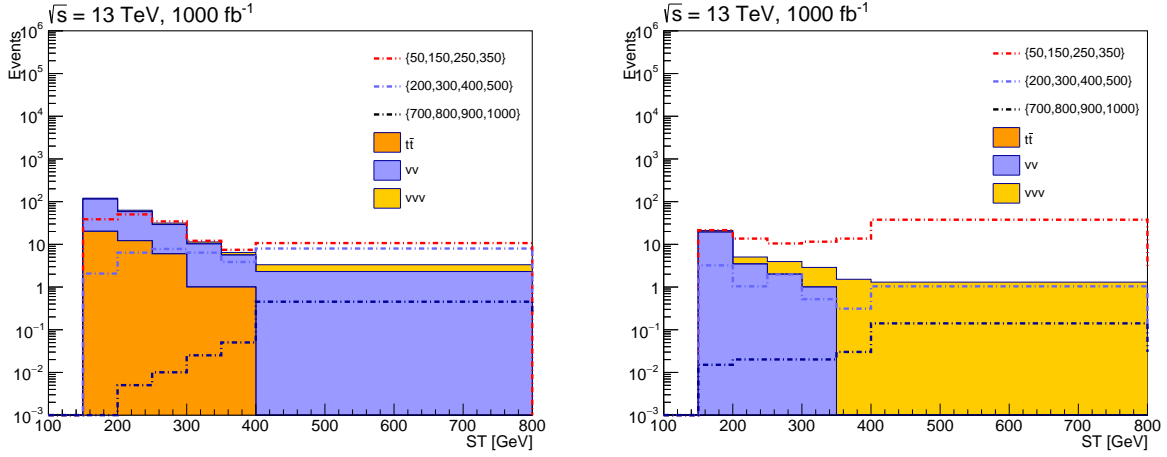
Figure 9.7: ST distribution for the expected number of events for $1000\,fb^{-1}$ luminosity, for the most relevant backgrounds (stacked) and for three different signal samples, dashed lines overlaid on top of the backgrounds. The distribution on the left is for the eee channel and the distribution on the right is for the $\mu\mu\mu$ channel.

9.2 VBF channel production

As mentioned before, the VBF topology is characterized experimentally by the presence of two highly energetic jets, with a large η gap, in opposite hemispheres of the detector volume, and large reconstructed dijet mass, which is defined in Equation 9.1 [72]. This technique has allowed to study difficult experimental regions, in mainly in searches for supersymmetry, and also study the production of new signal processes, considering dominant production through electroweak processes, because preferential couplings to this sector. Also, it have been proposed to study the production of Z' bosons and HN, as it was previously mentioned.

$$m(j_1, j_2) = \sqrt{2 p_T^{j_1} p_T^{j_2} \cosh(\eta_{j_1} - \eta_{j_2})} \tag{9.1}$$

Scenarios where the mass difference between the Majoron and the lightest neutrino (N_e) is 100 GeV ($\Delta m(N_e, J) = 100$ GeV) and where the following mass differences hold: $\Delta m(N_e, J) = \Delta m(N_e, N_\mu)$ = $\Delta m(N_\mu, N_\tau)$, were once again considered. The complete mass spectra explored in the analysis, is presented in Table 9.6. The signal samples simulation considered the processes: p p $\rightarrow \tau^-$ J τ^- j j , p p $\rightarrow \mu^-$ J μ^- j j and p p $\rightarrow e^-$ J e^- j j.

The syntax used to produced the signal samples in MadGraph is presented next:

```
> import model SM_HeavyN_UFO
> define lepton = e- mu- ta-
> define lepton~ = e+ mu+ ta+
> define neutrino = ve vm vt
> define neutrino~ = ve ~ vm ~ vt ~
> define p = u d u~ d~
> generate p p > lepton  j0 lepton j j
```

Table 9.6: Number of events produced for the analyzed mass spectra.

$\{m(J), m(N_e), m(N_\mu), \text{ and } m(N_\tau)\}$	Number of events
$\{50, 150, 250, 350\}$	200.000
$\{200, 300, 400, 500\}$	200.000
$\{700, 800, 900, 1000\}$	200.000

Figure 9.8 (left) shows the production cross section as function of the N_τ mass. The distribution before decay (blue) and for the process associated to the theoretical calculation performed in this project (see Figure 7.1) (yellow), are presented. In Figure 9.8 (right) is presented a comparison for the production cross sections between two possible VBF processes. Note that the process $pp > \tau N_\tau jj$, which has been studied at the LHC considering the N_τ stable, has a larger cross section. Nevertheless, the model presented in this project has not been studied at the LHC so far. The fact that the HNs are unstable, result and in a larger lepton multiplicity in the final state and large p_T^{miss} due to the associated Majoron.
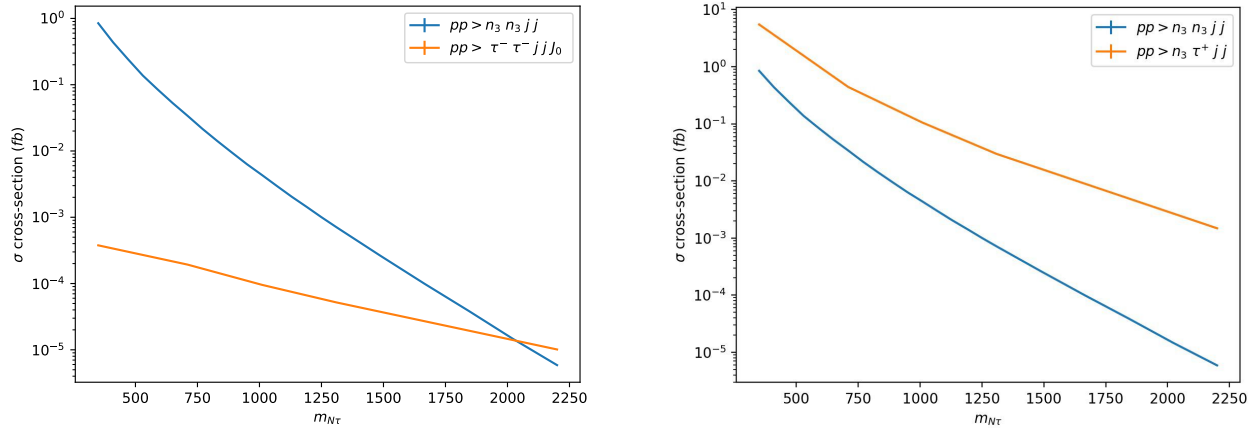

Figure 9.8: Left: (Blue) Cross section as function of m(N_τ) considering production of stable neutrinos. (Yellow) Cross section considering Majoron radiation and non stable neutrinos. Right: (Blue) Cross section as function of m(N_τ) considering production of stable neutrinos. (Yellow) Cross section considering Tau production with two jets and a stable neutrino.

Figure 9.9 shows that the signal samples follow the nature proper to the VBF topology. This variable helps to distinguish the signal from the background processes, which are mainly detected at the barrel region of the detector. Thus, the η distribution for the jets is centered at zero. Note that this distribution shows potential to remove as most background events as possible. Additionally, Figure 9.10 shows the restriction made, at generation level, over the η separation between the two produced jets $|\Delta\eta(j_1, j_2)| > 3.8$. It is worth noticing that this distribution shows the behavior associated to VBF topology for the signal events. Hence, this variable shows

a potentially interesting behavior to eliminate background events. Figure 9.11 shows the p_T^{miss} distribution for both signal and background events.
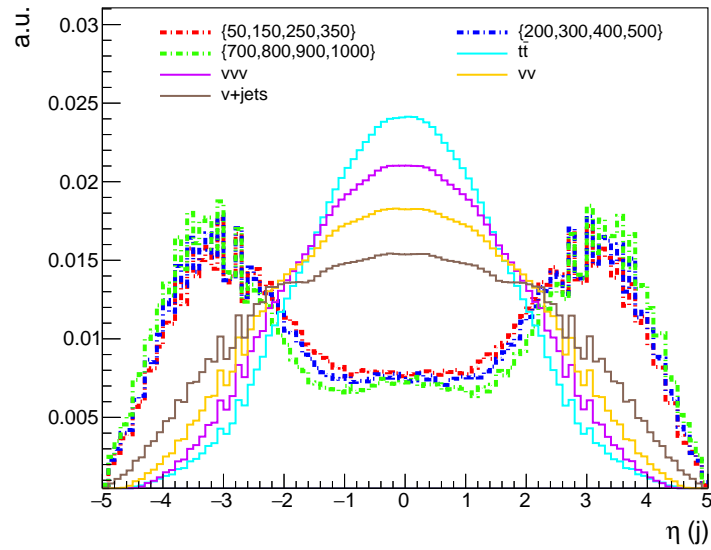

Figure 9.9: η distribution for the jets. The notation for the signal samples correspond to $\{m(J), m(N_e), m(N_\mu), m(N_\tau)\}$.
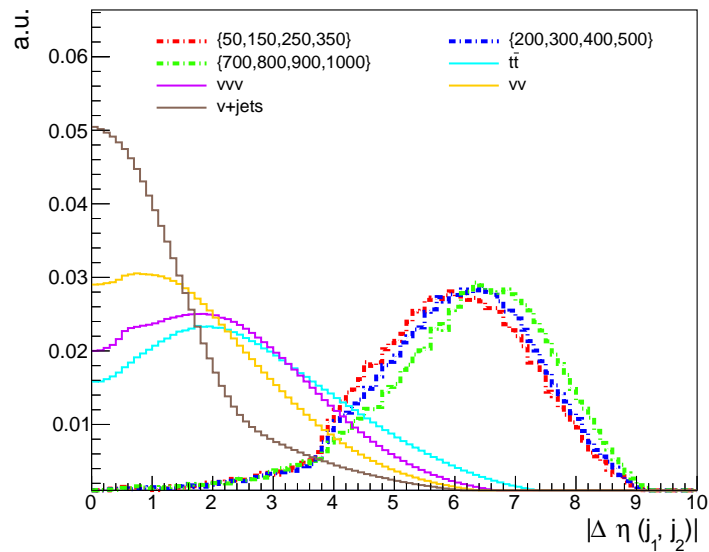

Figure 9.10: $|\Delta\eta|$ distribution for the jets. The notation for the signal samples correspond to $\{m(J), m(N_e), m(N_\mu), m(N_\tau)\}$.
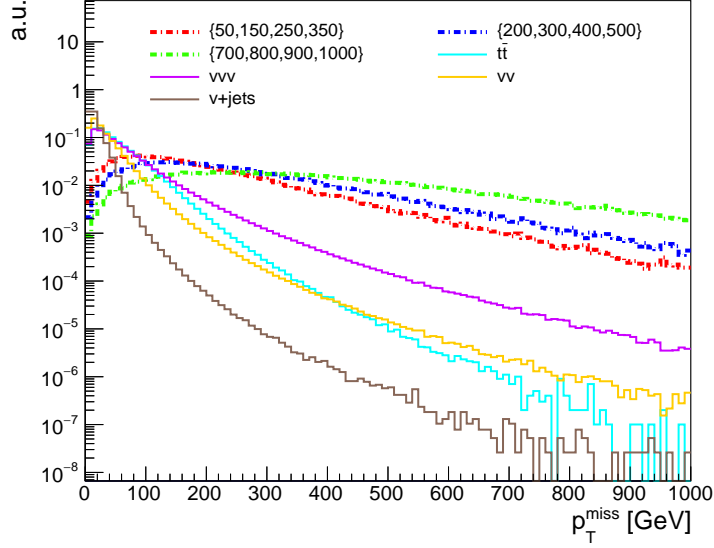
Figure 9.11: p_T^{Miss} distribution. The notation for the signal samples correspond to $\{m(J), m(N_e), m(N_\mu), m(N_\tau)\}$.

As the events in the VBF channel require similar p_T and p_T^{miss} requirements to those of the W-channel, the S_T distribution has been also explored. Figures 9.12 show the transverse momentum distributions for both electrons and muons, showing an interesting behavior that can help us to eliminate some background events. Additionally, Figure 9.13 shows the ST distribution of the channel, which functions as an interesting variable to distinguish between background and signal events due to the separations between the values given for each of the considered processes.
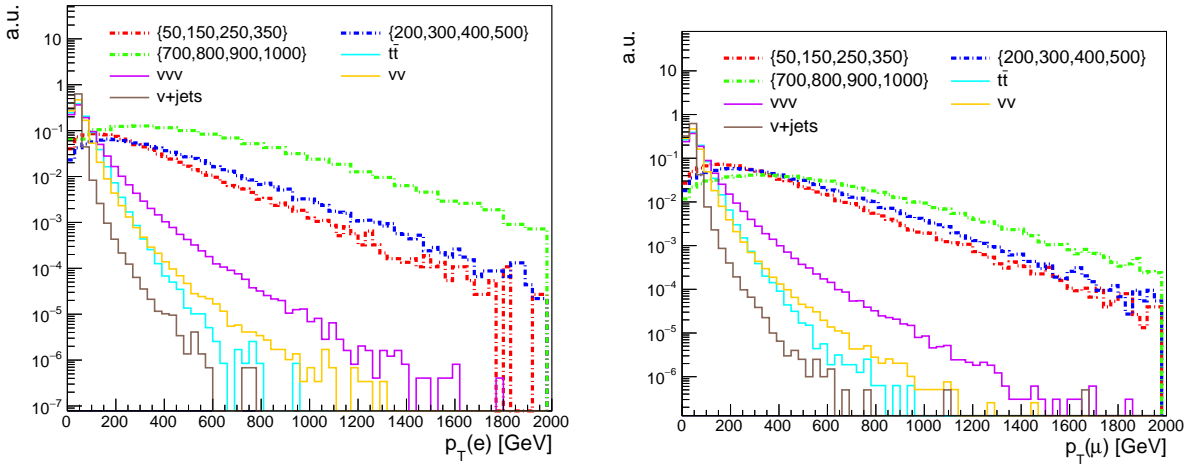

Figure 9.12: p_T distributions, in logarithmic scale, for the electrons (Left) and muons (Right).The notation for the signal samples correspond to $\{m(J), m(N_e), m(N_\mu), m(N_\tau)\}$.

66
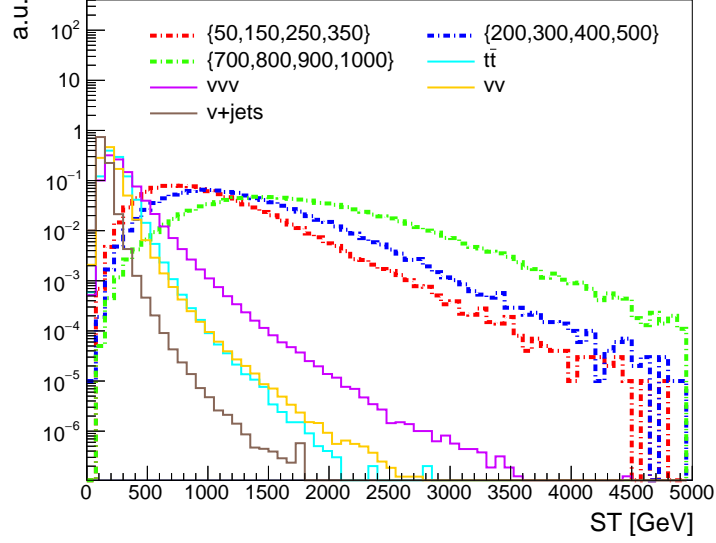
Figure 9.13: ST distribution in logarithmic scale. The notation for the signal samples correspond to $\{m(J), m(N_e), m(N_\mu), m(N_\tau)\}$.

Table 9.7: Topological selections

Criteria	Selections
p_T^{miss}	> 150 GeV
$N(b-jets)$	0
$p_T(b-jets)$	> 30 GeV
$|\eta(b-jets)|$	< 2.5

Table 9.8: VBF selections

Criteria	Selections
$N(j)$	≥ 2
$p_T(j)$	> 30 GeV
$|\eta(j)|$	< 2.5
$\eta(j_1) \cdot \eta(j_2)$	< 0
$|\Delta\eta(j_1, j_2)|$	> 5.5

The selection criteria given in Table 9.7 were aimed to remove events with low p_T^{miss} values and b-jet production. The established p_T^{miss} value has been set to 150 GeV due to the presence of the heavy neutrino states in the VBF topology, and to remove the backgrounds coming from SM electroweak processes. The restrictions over the b-jets are aimed to eliminate any possible QCD background, specially those coming from the hadronization processes of the jets, as well as

those coming from the hadronic decays of the W bosons. Table 9.8 shows the set of cuts used to optimize the di-jet mass value given the VBF topology. Hence, we required the pair of jets to have proper η and p_T values, such that they have the minimum reconstruction requirements given the experimental constrains of the CMS detector.

Table 9.9: Percentage cumulative efficiencies for the signals and backgrounds after every cut.

Signals						
{m(J), m(N$_1$), m(N$_2$), m(N$_3$)}	ϵ_I	ϵ_{II}	ϵ_{III}	ϵ_{IV}	ϵ_V	ϵ_{VI}
{200, 300, 400, 500}	65.985	30.128	4.852	4.476	4.215	9.354
{700, 800, 900, 1000}	82.519	38.423	7.028	5.162	6.887	11.311
{50, 150, 250, 350}	49.733	21.808	3.183	3.73	2.052	6.586
Backgrounds						
Sample	ϵ_I	ϵ_{II}	ϵ_{III}	ϵ_{IV}	ϵ_V	ϵ_{VI}
www	4.444	0.077	0.012	0.017	0.109×10^{-2}	0.17×10^{-2}
zzw	6.658	0.120	0.008	0.010	0.156×10^{-2}	0.24×10^{-2}
zzz	5.683	0.083	0.003	0.002	0.168×10^{-2}	0.26×10^{-2}
wwz	8.316	0.115	0.015	0.018	0.132×10^{-2}	0.16×10^{-2}
$t\bar{t}$	0.657	0.029	0.004	0.00639727	0.209×10^{-3}	0.382×10^{-3}
z+jets	0.102	0.001	1.621e-05	1.621e-05	5.400×10^{-3}	-
w+jets	0.051	0.001	0.133×10^{-3}	0.00019115	-	-
ww	0.799	0.014	2.096×10^{-3}	3.184×10^{-3}	5.6×10^{-5}	0.12×10^{-3}
zz	1.457	0.018	0.48×10^{-3}	0.39×10^{-3}	0.14×10^{-3}	0.22×10^{-3}
wz	1.251	0.024	1.431×10^{-3}	2.497×10^{-3}	4.061×10^{-5}	8.122×10^{-5}

After analyzing the distributions given before the selection criteria given in Tables 9.7 and 9.8 were applied to reduce background contamination while keeping as much signal events as possible. After applying these selections, we considered two different extra channels, {e,e} (CH1) and {μ,μ} (CH2) given the diagonal couplings between leptons and neutrinos. The cumulative efficiencies of the different set of selections are presented in Table 9.9. Efficiency ϵ_I corresponds to the events passing the selections reported on Table 9.7. ϵ_{II} corresponds to events after passing the selections given in Tables 9.7 and 9.8, while ϵ_{III-IV} correspond to events passing selections on Tables 9.7 and 9.8 given the production of a single electron or muon, together with a stable neutrino as illustrated in Figure 9.8. Furthermore ϵ_{V-VI} correspond to events passing the selections given on Tables 9.7 and 9.8, as well as the requirements of CH1 and CH2. It is important to note that the selection criteria for this study shows good potential to discriminate signal from background, showing that this analysis can be potentially performed at the LHC. However, a potential discovery of a Majoron in this channel would require large luminosity values to reach the 5σ statistical significance of a hypothetical discovery. Hence, this type of analysis might require luminosity values larger than $1000 fb^{-1}$, namely the $3000 fb^{-1}$ expected to be collected by the end of the LHC physics program.

10. Conclusions

This work provides tree-level calculations of the production matrix elements of a stable Majoron radiated from massive neutrino states, whose masses are considered to be in the Seesaw limit and generated by the type 1 Seesaw mechanism, in three different channels: DY, VBF and W-mediated. Then, a preliminary phenomenological study of the hypothetical production and detection of this particle was successfully carried in the W and VBF channels, showing the promising character of the model for future studies with real data from the CMS and ATLAS detectors. This preliminary phenomenological study allowed to establish event selection criteria to reduce the background while keeping most of the signal in the W and VBF channels.

As a future study it is recommended to explore the DY channel, as well as loop induced production of a Majoron in the Seesaw limit. Secondly, a similar phenomenological study exploring the studied channels while considering non diagonal couplings between leptons and neutrinos is suggested. Furthermore, it is recommended to study the hypothetical production of heavy neutrinos and Majorons in future colliders such as the International Linear Collider or the Future Circular Collider.

Finally, the work conducted in this dissertation is associated with an article that will be sent to a peer reviewed journal in the following months.

Bibliography

[1] G. Ardila. A phenomenological study of a z' boson in the jj+ll channel with an intermediate heavy neutrino state using vector boson fusion processes. Bsc. thesis, Universidad de Los Andes, 2017.

[2] V. Heine. *Group Theory in Quantum Mechanics*. Wiley, 2010.

[3] M. Frasca. Proof of triviality of $\lambda\phi^4$ theory. *International Journal of Modern Physics A*, 2007.

[4] A. R. Vieira et al. Naturalness and theoretical constraints on the higgs boson mass. *International Journal of Theoretical Physics*, 2013.

[5] G. C. Nayak. Matter-antimatter asymmetry of the universe and baryon formation from non-equilibrium quarks and gluons. *arXiv:1909.05640 [physics.gen-ph]*, 2019.

[6] G. Fantini et al. The formalism of neutrino oscillations: an introduction. *arXiv:1802.05781 [hep-ph]*, 2018.

[7] G. Esposito. An introduction to quantum gravity. *arXiv:1108.3269 [hep-th]*, 2011.

[8] Y. Shadmi. Introduction to supersymmetry. *CERN Yellow Reports Vol. 3: Proceedings of the 2014 European School of High-Energy Physics*, 2016.

[9] S. Raby. Grand unified theories. *arXiv:hep-ph/0608183*, 2006.

[10] M. Dine. *Supersymmetry and String Theory*. Cambridge University Press, 2015.

[11] J. C. Romao J. W. F. Valle. *Neutrinos in High Energy Physics and Astroparticle Physics*. Wiley, 2015.

[12] T. Yanagida M. Fukugita. Barygenesis without grand unification. *Phys. LettB98*, 1986.

[13] R. D. Peccei Y. Chikashige, R. N. Mohapatra. Are there real goldstone bosons associated with broken lepton number? *Phys. LettB98*, 1981.

[14] M. Schwartz. *Quantum Field Theory and The Standard Model*. Cambridge University Press, 2014.

[15] The IceCube Collaboration. The icecube neutrino observatory: Instrumentation and online systems. *Journal of Instrumentation*, 2017.

[16] The CMS Collaboration. The cms experiment at the cern large hadron collider. *Journal of Instrumentation*, 2008.

[17] The ATLAS Collaboration. The atlas experiment at the cern large hadron collider. *Journal of Instrumentation*, 2008.

[18] S. Rappoccio. The experimental status of direct searches for exotic physics beyond the standard model at the large hadron collider. *Reviews in Physics*, 2019.

[19] L. Lee et al. Collider searches for long-lived particles beyond the standard model. *Progress in Particle and Nuclear Physics*, 2019.

[20] A. Florez et al. Probing the stau-neutralino coannihilation region at the lhc with a soft tau lepton and an isr jet. *Physical Review D*, 2016.

[21] A. Flórez et.al. Searching for new heavy neutral gauge bosons using vector boson fusion processes at the lhc. *Physics Letters B*, 2017.

[22] A. Flórez et.al. Anapole dark matter via vector boson fusion processes at the lhc. *Physical Review D*, 2019.

[23] A. Gurrola et al. Probing heavy spin-2 bosons with $\gamma\gamma$ final states from vector boson fusion processes at the lhc. *Physical Review D*, 2019.

[24] David. J Griffiths. *Introduction to elementary particles*. Wiley, 2008.

[25] F. Mandl & G. Shaw. *Quantum Field Theory*. Wiley, 2010.

[26] D. V. Schroeder M. E. Peskin. *An Introduction To Quantum Field Theory*. Westview Press, 2016.

[27] M. Thomson. *Modern Particle Physics*. Cambridge University Press, 2013.

[28] P. B. Pal A. Lahiri. *A First Book On Quantum Field Theory*. Alpha Science, 2005.

[29] M. Kaku. *Quantum Field Theory: A Modern Introduction*. Oxford University Press, 1993.

[30] D. Goldberg. *The Standard Model In A Nutshell*. Princeton University Press, 2017.

[31] T. Lancaster & S. Blundell. *Quantum Field Theory For The Gifted Amateur*. Dover Publications, 2007.

[32] M. Maggiore. *A Modern Introduction to Quantum Field Theory*. Oxford University Press, 2005.

[33] K. Kumericki. Feynman diagrams for beginners. *arXiv:1602.04182 [physics.ed-ph]*, 2016.

[34] M. Srednicki. *Quantum Field Theory*. Cambridge University Press, 2007.

[35] W. Greiner et. al. *Field Quantization*. Springer-Verlag Berlin Heidelberg, 1996.

[36] J. J. Aubert et.al. Experimental observation of a heavy particle j. *Physical Review Letters*, 1974.

[37] J. E. Augustin et. al. Discovery of a narrow resonance in e^+e^- annihilation. *Physical Review Letters*, 1974.

[38] B. Grinstein. Introductory lectures on qcd. `https://cds.cern.ch/record/935622/files/p27.pdf`. Accessed: 2020-06-15.

[39] H. Georgi. *Lie Algebras In Particle Physics: From Isospin to Unified Theories*. Westview Press, 1999.

[40] W. Greiner et. al. *Quantum Chromodynamics*. Springer, 2007.

[41] H. Kleinert. *Particles And Quantum Fields*. World Scientific Publishing Company, 2016.

[42] C. Quigg. *Gauge theories of the strong, weak and electromagnetic interactions*. Princeton University Press, 2013.

[43] M. L. Mangano. Introduction to qcd. `https://cds.cern.ch/record/454171/files/p41.pdf`. Accessed: 2020-06-20.

[44] C. Wu et.al. Experimental test of parity conservation in beta-decay. *Physical Review*, 1969.

[45] B.R Holstein W.C Haxton. Neutrino physics. *American Journal of Physics*, 2000.

[46] M. Tanabashi et al. (Particle Data Group). The review of particle physics. *Physical Review D*, 2018.

[47] J. J. Tresher. Lep: Machine and experiments. *In: Kotthaus R., Kühn J.H. (eds) XXIV International Conference on High Energy Physics.*, 1989.

[48] S. Holmes. Remembering the tevatron: The machine(s). *arXiv:1109.2937 [physics.acc-ph]*, 2011.

[49] S. Weinberg. Physical processes in a convergent theory of the weak and electromagnetic interactions. *Physical Review Letters*, 1971.

[50] Paul Langacker. *The Standard Model and Beyond*. CRC Press, 2017.

[51] S.M. Bilenky et al. Absolute values of neutrino masses: Status and prospects. *Physics Reports*, 2003.

[52] P. Langacker et al. Neutrino physics. *arXiv:hep-ph/0506257v1*, 2005.

[53] E. Akhmedov et al. Seesaw mechanism and structure of neutrino mass matrix. *Physics Letters B*, 2000.

[54] C. Garcia-Cely J. Heeck. Neutrino lines from majoron dark matter. *Journal of High Energy Physics*, 2017.

[55] H. H. Patel J. Heeck. The majoron at two loops. *Physical Review D*, 2019.

[56] A.Leike. The phenomenology of extra neutral gauge bosons. *Physics Reports*, 1999.

[57] P. Langacker. The physics of heavy z' gauge bosons. *Reviews Of Modern Physics*, 2009.

[58] A. Pilaftsis. Astrophysical and terrestrial constraints on singlet majoron models. *Physical Review D*, 1994.

[59] C. P. Burgess. Goldstone and pseudo-goldstone bosons in nuclear, particle and condensed-matter physics. *Physics Reports*, 2000.

[60] I. R. Kenyon. The drell-yan process. *Reports on Progress in Physics*, 1982.

[61] A. Delannoy et al. Probing dark matter at the lhc using vector boson fusion processes. *Physical Review Letters*, 2013.

[62] B. Dutta et al. Vector boson fusion processes as a probe of supersymmetric electroweak sectors at the lhc. *Physical Review D*, 2013.

[63] J. Brooke et al. Vector boson fusion searches for dark matter at the lhc. *Physical Review D*, 2016.

[64] W. Rodejohann H. Päs. Neutrinoless double beta decay. *New Journal of Physics*, 2015.

[65] N. Vergara. Theoretical and phenomenological study for the production of heavy neutrinos and majorons at the lhc. Bsc. thesis, Universidad de Los Andes, 2020.

[66] T. McCauley T. Sakuma. Detector and event visualization with sketchup at the cms experiment. *Journal of Physics: Conference Series*, 2014.

[67] CERN cms experiment. `https://cms.cern/detector`. Accessed: 2020-08-19.

[68] Cms experiment: Muon detectors. `http://cms.web.cern.ch/news/muon-detectors`. Accessed: 2020-08-19.

[69] M. Dunford M. Schott. Review of single vector boson production in pp collisions at $\sqrt{s} = 7$ tev. *The European Physical Journal C*, 2016.

[70] B. Muratori W. Herr. Concept of luminosity. *Accelerators and Colliders. Landolt-Börnstein - Group I Elementary Particles, Nuclei and Atoms (Numerical Data and Functional Relationships in Science and Technology)*, 2013.

[71] Record luminosity: well done lhc. `https://home.cern/news/news/accelerators/record-luminosity-well-done-lhc`. Accessed: 2020-08-20.

[72] N. Cardona. Search for pure higgsino dark matter at the lhc using vector boson fusion. Bsc. thesis, Universidad de Los Andes, 2020.

[73] A. Denner. Compact feynman rules for majorana fermions. `https://www.desy.de/~gudrid/teaching/WIS1718/majorana-rules.pdf`. Accessed: 2020-01-24.

[74] W. Rodejohann. Phenomenological aspects of majorana neutrino mass matrices. Ph.d thesis, Universität Dortmund, 2001.

[75] Adam Alloul, Neil D. Christensen, Céline Degrande, Claude Duhr, and Benjamin Fuks. FeynRules 2.0 — A complete toolbox for tree-level phenomenology. *Computer Physics Communications*, 185:2250–2300, 2014.

[76] Johan Alwall, Michel Herquet, Fabio Maltoni, Olivier Mattelaer, and Tim Stelzer. MadGraph 5: Going beyond. 2011(6):128, June 2011.

[77] Torbjörn Sjöstrand, Stephen Mrenna, and Peter Skands. A Brief Introduction to PYTHIA 8.1. *Computer Physics Communications*, 178(11):852–867, June 2008.

[78] S. Ovyn, X. Rouby, and V. Lemaitre. Delphes, a framework for fast simulation of a generic collider experiment. *[physics:hep-ph]*, April 2010.

[79] A. Florez et al. Expanding the reach of heavy neutrino searches at the lhc. *Physics Letters B*, 2018.

[80] CMS Collaboration. Search for heavy neutrinos and third-generation leptoquarks in hadronic states of two τ leptons and two jets in proton-proton collisions at $\sqrt{s}=$ 13 tev. *Journal of High Energy Physics*, 2019.

[81] CMS Collaboration. Search for heavy neutral leptons in events with three charged leptons in proton-proton collisions at $\sqrt{s}=$ 13 tev. *Physical Review Letters*, 2018.

[82] CMS Collaboration. Search for supersymmetry with a compressed mass spectrum in the vector boson fusion topology with 1-lepton and 0-lepton final states in proton-proton collisions at $\sqrt{s}=$ 13 tev. *Journal of High Energy Physics*, 2019.